1-1-2017

Differential Activation Of Dead Box Rna Helicases Rhlb And Rhle By Hfq/srnas And Their Target Mrnas

Amit Kumar
Wayne State University,

Differential activations of DEAD box RNA helicases RhlB and RhlE by Hfq/sRNAs and their target mRNAs

by

AMIT KUMAR

THESIS

Submitted to the Graduate School

of Wayne State University,

Detroit, Michigan

in partial fulfillment of the requirements

for the degree of

MASTER OF SCIENCE

11th APRIL, 2017

MAJOR: CHEMISTRY (Biochemistry)

Approved by:

Andrew Feig 4/4/17

Advisor Date

Andrew Feig

DEDICATION

I dedicated this dissertation to my mother (Sudha Devi), my father (Vijay Shankar Upadhyay), my family members, my friend (Shirin Fatma), and my dissertation advisor, Professor Andrew L Feig. I would like to thank you all for your invaluable time, support, and guidance.

ACKNOWLEDGMENTS

I acknowledge, with my deepest gratitude, my advisor, Professor Andrew L. Feig for his constant encouragement, advice, and support over my seven years at graduate school, and for making this publication possible. I am thankful to him for his guidance and patience at times when I failed. I am thankful to him not only for teaching and guiding me to learn the laboratory and scientific skills and way of thinking but also, for teaching me the lessons which have made deep impact on me and will help me grow as a person throughout my professional and social life.

I would also like to sincerely express my gratitude to my thesis committee member, Professor Tamara Hendrickson for her invaluable time and support whenever I needed; Dr. Jared Schrader, for his time and for accepting to be my committee member. My special thanks to them for their understanding, being considerate, and for accommodating me in their busy schedules.

I would like to thank all my lab member who has helped me from the very beginning of my graduate school career at Wayne State University. Dr. Salim, Dr. Sanofar, Iresha, Dandan, Dr. Faner, Dr. Kern, Dr. Swett, Dr. Jane Phillip, Sonia, Danielle Anetterini, Faraz Khan, Brianna Jackman, and Adam Boyden. I thank them for accepting me as new member of Feig group, sharing their knowledge and enthusiasm towards science and, more importantly creating and supporting an amicable work environment.

My greatest gratitude goes to my close friends Chaithanya K Mummidisetty, Veeranna Yempally, Dr. Ram P Bora, Sudeshna Ganguly, Debashish Basu, Dr. Geetha Varakala, Rajesh Varakala, Dr. Saptarshi De, Syeda Fatima Sultana, Girish Sati, Chandra S Chimakurthy, Sarita Jena, Dr. Satish Garre, Karan Arora, Animesh Balse, Omkar Patkar, Pranoy Ghosh, Atul Singh and Susan White. These friends have always been there for me during my struggles and frustrations, giving me encouragement to move forward.

I would also like to express my gratitude to the Department of Chemistry, Wayne State University for providing me with the resources I needed. In addition, I am thankful to their teaching assistant system that I enjoyed and that improved my teaching skills immensely; I am a better and confident teacher now because of these experiences. Thanks also to Professor Ashok Bhagwat, Professor Tamara Hendrickson and Professor Christine Chow for giving me permission to use equipment in their lab as well as in the

department's RNA center. I would also like to extend my gratitude to our department office staffs, especially Melissa Barton for all her help and time.

Last but not the least; I would like to thank my dear parents, my fiancée Shirin Fatma, my family, and relatives for believing in me and sending me far from home to pursue my career. They have loved and supported me throughout my entire life, and I am forever indebted to them for all the sacrifices they have made for me. Thank you.

TABLE OF CONTENTS

LIST OF TABLES

LIST OF FIGURES

Chapter 1: Small regulatory RNAs in bacteria: introduction, functions, and mechanism

Small RNAs (sRNAs) have emerged as important players in bacterial gene regulation. Studies over more than a decade have led to the discovery of more than one hundred and fifty validated and putative sRNAs in *E. coli* alone.[1-2] Advancements in technology have further helped the discovery of new sRNAs.[3-5] sRNAs have been established as major contributors to the swift regulation of genes required under the various stresses incurred due to changing environmental conditions between hosts and surroundings. Bacteria face such conditions frequently over their lifetimes, and unlike long term adaptations like antibiotic resistance, which involves the acquisition and/or mutation of genes, rapid adaptation is required for survival. Adaptations to rapidly changing conditions such as changes in temperature, and concentration of salts and oxygen require fast and fine tuning of the existing system by altering expression and regulation. Hence, sRNAs add another layer of gene regulation in addition to the regulatory proteins.

1.1.1 Introduction and function

sRNA is a rapidly expanding class of non-protein posttranscriptional regulators of bacterial gene expression. As their name implies, these generally do not code for proteins. Few exceptions include the SgrS gene that encodes for a peptide SgrT,[6] SR1 in *B. subtilis* [7] and RNAIII in *S. aureus*.[8] Several types of sRNAs have been identified over the years including riboswitches, thermo-sensors, cis-acting and trans-acting sRNAs, and crRNA of the CRISPR-Cas system. Previously thought to be solely coded in intergenic regions, sRNAs have surprised us with their widely distributed origins. sRNAs originating from 5' or 3' untranslated regions of the mRNA, or near transcriptional termination regions have also been identified.[9-11] Many sRNAs are generated

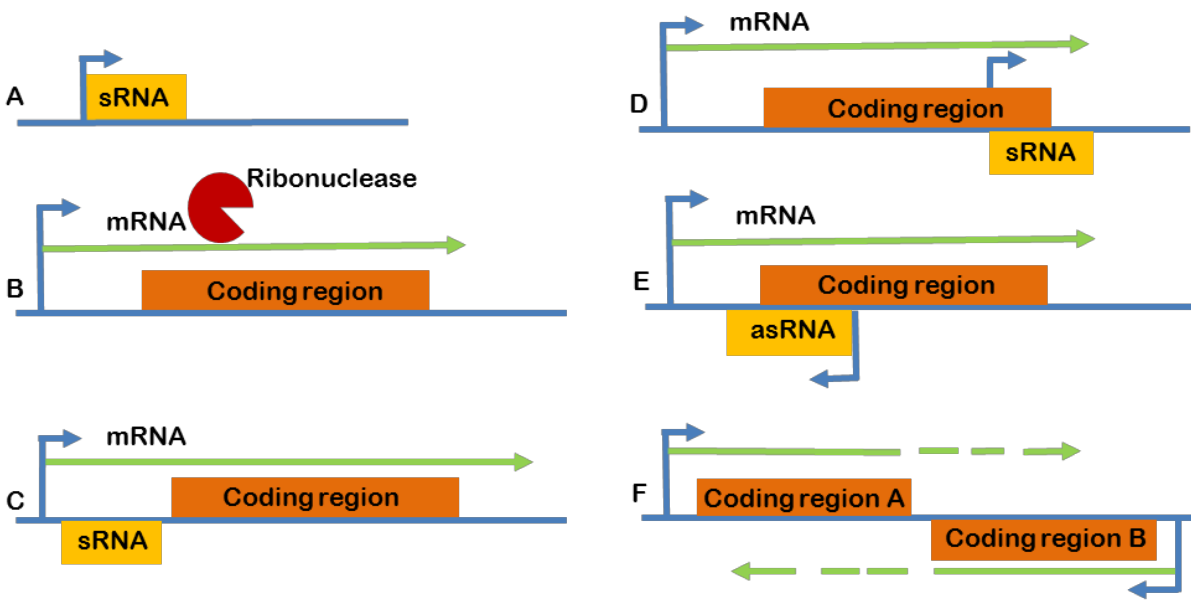

Fig 1.1: Origins of sRNAs from DNA/RNA with respect to their target genes. (A) a typical trans acting sRNA expressed from loci different than its target gene. Riboswitch-sRNA would fall in this category. (B) Small RNAs produced by the processing of an mRNA transcript or a poly-cistronic pre-tRNA transcript. Processing here implies immature termination or processing of the transcripts by one or more ribonuclease producing non-translating fragments. These fragments could be from 5'/3'UTR or from anywhere in a coding sequence, and they may act as trans acting small RNA targeting other genes. This class would include the 5' riboswitches that induces premature transcription termination of the adjacent downstream coding gene and the premature transcript fragment display sRNAs like activity. (C) and (D) Represent the cis-acting regulatory RNA coding sequence embedded towards the 5' region and 3' region of a protein coding gene respectively. This class would also include 3' riboswitches (E) The presence of small RNA on the antisense strand of a coding gene, commonly known as cis-acting antisense RNA. The position of small RNA could be anywhere in/overlapping to the target ORF. (F) Anti-sense regulatory RNAs originated after processing of transcripts of protein coding genes expressed in opposite directions, from complementary DNA strands. The transcripts have complementary overlapping region. Blue line (DNA), blue arrow (promoter), yellow box (sRNA gene), green boxes (mRNA or polycistronic tRNA gene as shown), light Green arrow (non-small RNA transcript from the corresponding gene) and red pacman (ribonucleases which process the transcripts) [17]

as byproducts of natural processing of mRNAs *in vivo*.[12-13] Premature transcription termination prevents the expressions of downstream ORFs and the transcript generated, in some cases, can act as sRNA.[14] Transcript expression from the same or antisense DNA strands with overlapping regions could also give rise to anti-sense regulatory RNAs.[10] Recent studies have shown that specific tRNA fragments (tRFs) sequester sRNAs by base pairing. Bacterial tRFs that act like sRNAs have shown higher affinity towards other sRNAs (RyhB and RybB sRNAs used for the study).[3] In bacteria tRFs mediate the regulation by sequestering sRNAs under normal conditions.

Similar to the diversity of their origins **(Fig 1.1)**[15], sRNAs seem to adapt to diverse operational mechanisms as far as modes of gene regulations are concerned. tRFs are also known to exist in human cells. However, unlike bacterial tRFs, the genes are regulated by tRFs base pairing to mRNAs[16] or by promoting cell proliferation.[17]

1.1.2 Mechanisms of sRNAs mediated gene regulation

sRNAs are divided into two classes based on the position of target genes with respect to the position of sRNA encoding region: cis-acting sRNAs and trans-acting sRNAs. RNAs from both classes have adapted to different mechanisms by which they achieve regulatory outcomes (**From this point, the term sRNA will be used to refer specifically to trans-acting small RNAs**). Cis-acting small RNAs affect the gene of the same loci. For instance, riboswitches which were classically recognized as cis-acting regulatory elements present in 5' UTRs, regulate the expression of the adjacent downstream open reading frames (ORFs). Riboswitches have an aptamer region and an expression platform. The aptamer motifs can bind to metabolites or small molecules (ligands) and change the confirmation of the expression platform, which results in transcriptional or translational modulation of the gene **(Fig 1.2A** left and middle panel**)**.[18-19] However, recent discoveries have established dual roles for riboswitches, where a single small RNA is both a cis-acting riboswitch and a trans-acting sRNA. Such examples were found in *Listeria monocytogenes and Clostridium acetobutylicum* where the riboswitch present towards the 3' end of an ORF regulates the expression of upstream adjacent genes. This riboswitch regulates the expression of an anti-sense RNA which in turn interacts with the target gene; hence, the riboswitch indirectly controls the target gene. [20-21] Reports suggest that riboswitches can also be a part of an sRNA which, in the absence of its binding ligand act as an sRNA and regulate the gene by sequestering the RNA binding response regulator and hence downregulating the gene. When

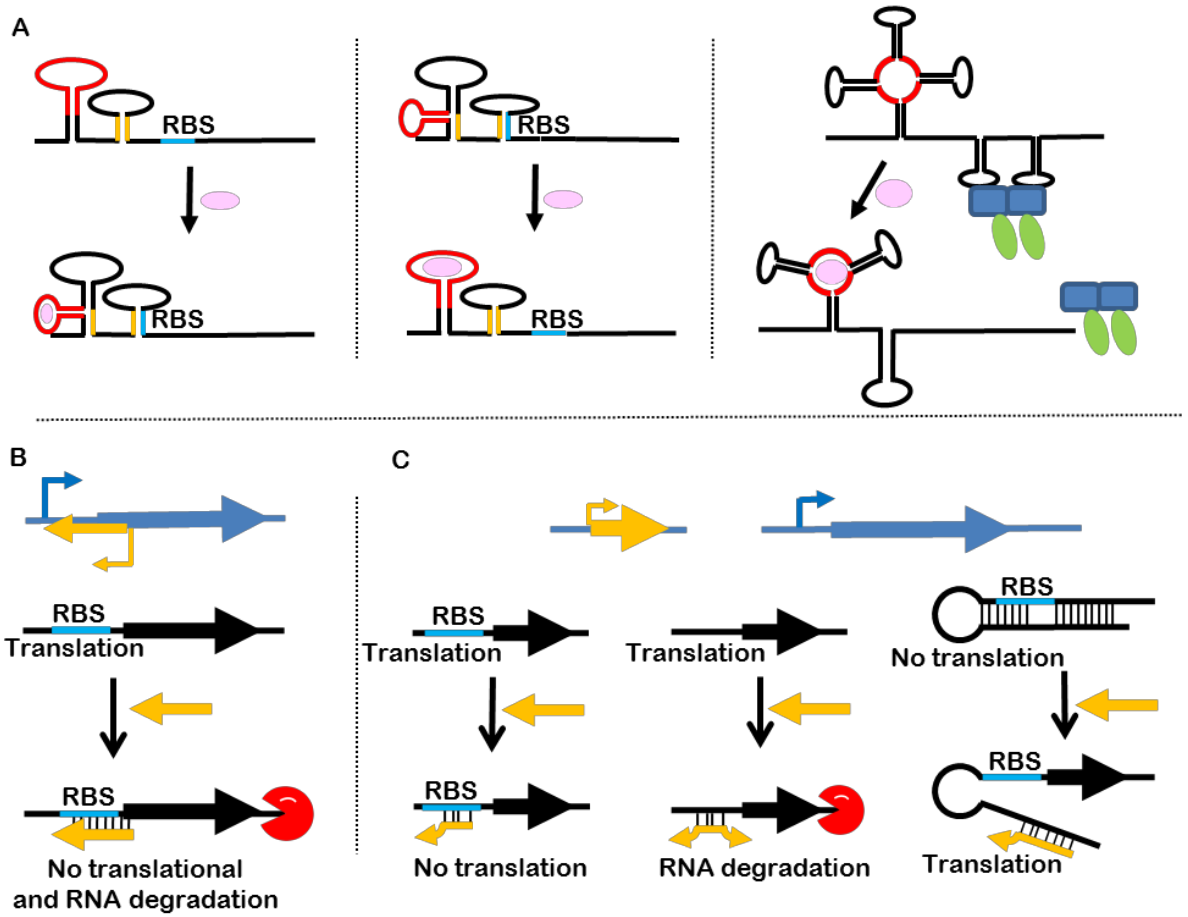

Fig 1.2: Mechanisms of action used by sRNAs in bacteria to modulate the regulatory outcomes. **(A)** Left and middle panel: A typical cis-acting riboswitch with an aptamer region (red) which binds with the ligand. Ligand binding to aptamer region results in the structural region (yellow) which either releases the previously occluded ribosome binding site (left panel) or vice-versa (middle panel) and hence results in either downregulation or upregulation of adjacent downstream gene. Right panel shows presence of a riboswitch motif 5' to the seed sequence of an sRNA molecule. In absence of ligand the sRNA sequesters the regulator protein and hence down regulating the target gene. Upon ligand binding conformational rearrangement results in to the release of regulator proteins and hence upregulating the expression. **(B)** A typical cis-acting small RNA which binds to its target with perfect complementarity which leads to translational repression by occluding the RBS or degradation of mRNA. **(C)** Trans-acting small RNA (sRNA) expressed from a loci different than its target genes loci. Upon abundant expression, sRNAs bind to their target mRNAs (often more than one targets) and either down-regulate the genes by occluding the RBS or mRNA degradation or up-regulate by releasing the pre-occluded RBS. (ribosome binding site, RBS, shown in light blue; ligand as pink circle; regulator protein shown as dimer blue box and green circle; blue line and thick arrow indicates the genomic DNA and the gene respectively; black lines and thick arrow indicates the transcript and translatable portions respectively; yellow arrows represents small RNAs' location when touching the blue line and free yellow arrow represents the sRNA transcript; promoters of small RNA and coding genes are shown by the horizontal arrow on the stick of matching colors) [22-26]

the ligand is present, riboswitch binds to the ligand and restructures the sRNA half in such a way that the motif required to sequester the RNA-binding regulator does not form, thus rendering the

target gene upregulated **(Fig 1.2A** right panel**)**.[22-24] Other cis-acting small RNAs affect the gene of the same loci but are coded on the antisense strand of its target gene, also known as antisense RNA (asRNA). asRNA base pairs perfectly to its target mRNA. Upon binding to its target sequence, an asRNA can lead to translational up/down regulations or mRNA degradation **(Fig 1.2B)**.[25-27]

sRNAs (trans acting small RNAs), on the other hand, are coded on entirely different and independent loci than their target mRNAs. Hence, base pairing between sRNAs and their target mRNAs are imperfect. Once bound to their target these sRNAs operate like cis-acting RNAs **(Fig 1.2C)**.[26] The ability of sRNA to regulate their target mRNA by imperfect paring turns out to be an advantage, as one sRNA can target multiple mRNAs and modulate their expression simultaneously. The imperfect complementarity of sRNAs to their target mRNAs results in a complex regulatory network where an sRNA can target multiple genes and at the same time, a single gene can be targeted by multiple sRNAs (**Fig 1.3)**.[26]

Many membrane transporter proteins, sigma-factors, toxins and virulence genes fall under the category of the sRNA's targets. Despite many regulatory sRNAs having been discovered, the involvement of protein partners has also been speculated to bring regulatory outcomes. Proteins could contribute to the sRNA mediated regulatory pathway either directly by interacting with the sRNAs or indirectly via interaction with other proteins.

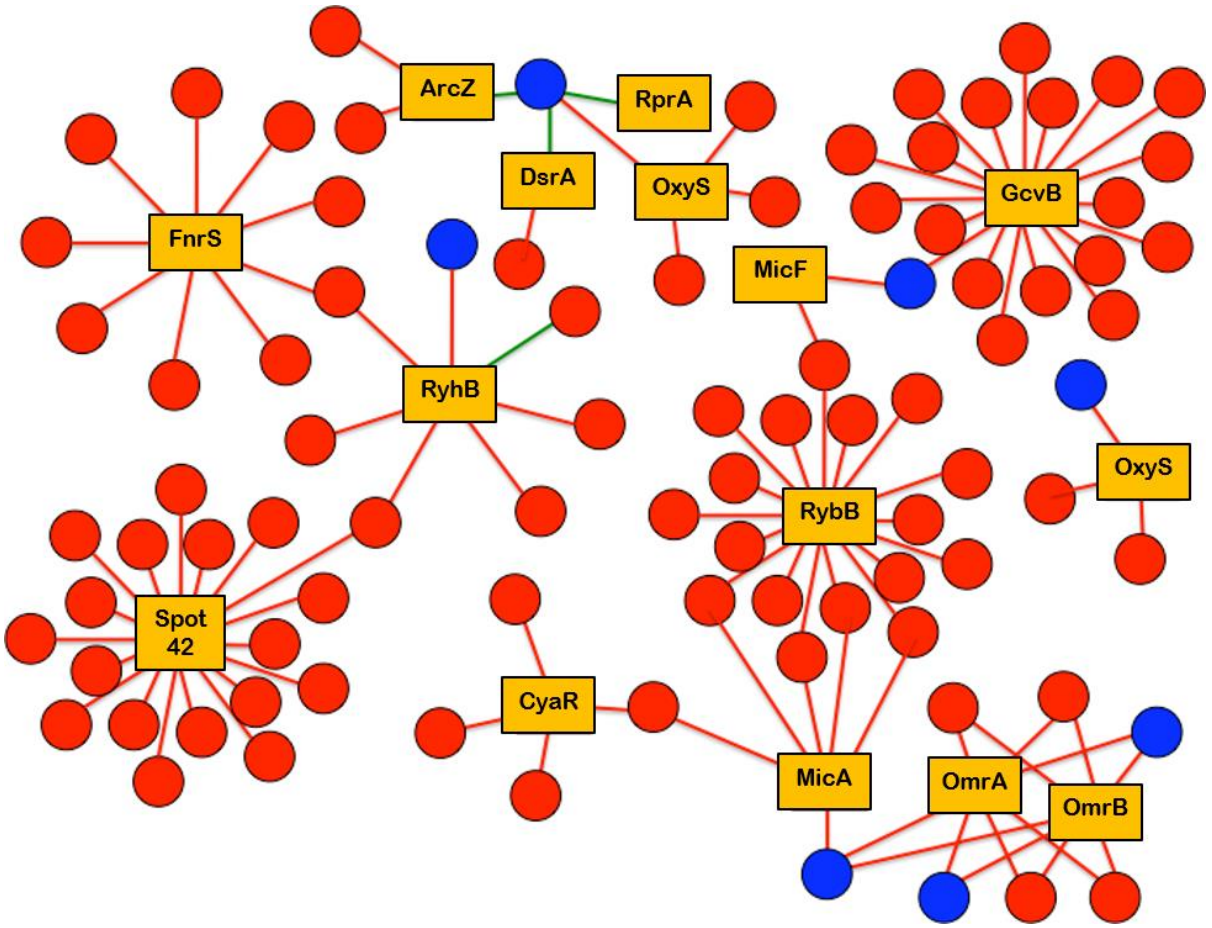

Fig 1.3: Schematic representation of the sRNA-mRNA mediated regulatory network; red circles: the mRNA targets, yellow box: sRNA, blue circles: the regulated gene which are transcription regulators, green lines: up-regulation of target gene and, red lines: indicates the down regulation of target gene. [26]

1.2 sRNA mediated regulations in *E. coli* require a protein partner: Hfq

Hfq is the most common protein partner of sRNA mediated regulation and has been widely studied.[28-33] It is required by most of the sRNAs in *E. coli* to perform their regulatory functions. Investigations to reveal plausible protein partners contributing directly or indirectly to sRNA mediated systems have revealed more than 30 proteins or protein complexes in interactions with Hfq.[34] Only a few of these Hfq-protein/complex interactions are known for their regulatory contributions so far and are discussed later. However, the interaction of sRNAs with proteins other

than Hfq have also been reported. Examples include ProQ and CsrA proteins, which are discussed in section 1.3 and 1.4.[35-37]

Initially identified as a host factor for bacteriophage Qβ RNA replication in *E. coli*, Hfq has established its role as a global regulator of sRNA mediated regulation in gram-negative bacteria.[31, 38-40] Hfq is a homo-hexameric protein, homologous to eukaryotic Sm/Lsm proteins. The N-terminal half of Hfq is highly structured and conserved, however the C-terminal half shows high

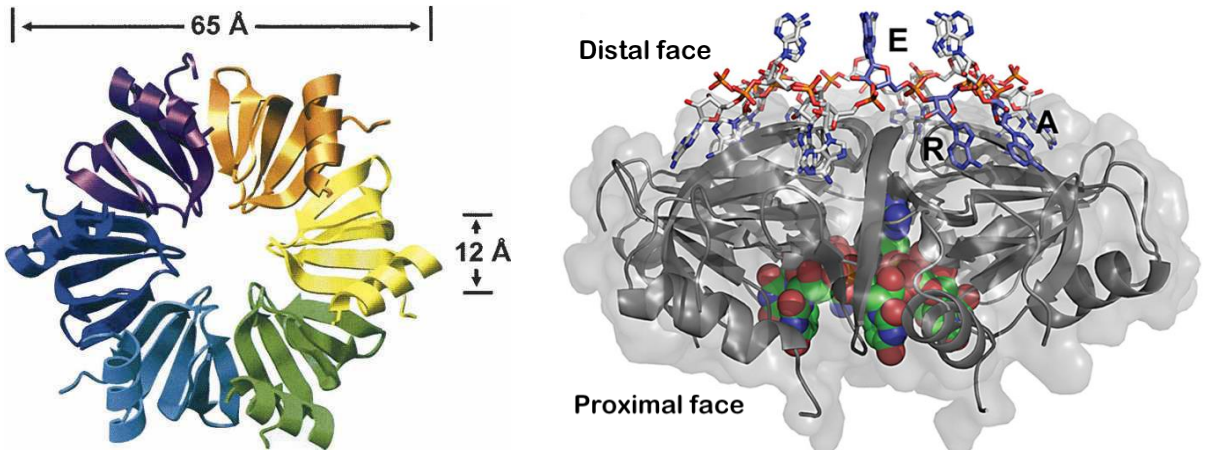

Fig 1.4: Hfq structures. (A) PDB ID : 1KQ2, (2) Hfq model reconstructed using two independent crystal structures 1KQ2 and 3GIB. Proximal face bind two A_9 molecules and the distal face binds AU_5G. Figure was prepared using Chimera.[43-45]

sequence and length variability among different bacterial species.[41] Also, the C-terminal region is predicted to be unstructured. Hfq deletion strains show reduced growth rate, increased stress sensitivity, reduced virulence to pathogenic strains, and alteration in the expression level of around 50 proteins.[42] The Hfq monomers arrange to form a doughnut shaped hexameric protein, with two distinct faces. Crystallographic and biochemical studies have confirmed that the proximal face binds to AU-rich sequence while the distal face binds to $(ARN)_X$ motifs **(fig 1.4)**.[43-45]

Dr. N. Salim's work suggests that the mRNA or sRNA might contact Hfq on both faces, to act as a bidentate ligand.[46] Recent studies have emphasized the contribution of rim residues facilitating sRNA-mRNA pairing. Also, the presence and the number of positively charged

arginine residues in the rim have been found to affect sRNA-mRNA annealing.[47-48] Schu *et al*., recently proposed a model like our two-point contact model where sRNA instead of mRNA contacts Hfq at two different points. According to the proposed models sRNA can (i) contact Hfq on proximal face using the poly-U tail and the second point of contact could be on the rim of Hfq; or, (ii) sRNA can contact on the proximal face using the poly-U tail and then wraps around to make a second contact on the distal face of Hfq **(Fig:1.5)**.[49] Nonetheless, the new model of sRNA making multi-point contact with Hfq supports the previously proposed multi-point contact model suggesting that an RNA molecule can make contacts with Hfq on more than one surfaces.[46] Binding of both the sRNA and mRNA to the Hfq results in a ternary complex, which facilitates the pairing of an RNA couple by increasing the proximity of partner RNAs and inducing some structural changes.[28] Most of the Hfq studies so far have focused on the more structured N-terminal half of Hfq while the truncated versions of Hfq (Hfq with first 65 and 76 amino acids) seem to act as full length Hfq as far as assisting the sRNA-mRNA pairing is concerned.[50] In a study where the *C. difficile* Hfq was constitutively expressed from a low copy number plasmid in the *Δhfq E. coli* strain, the *C. difficile* Hfq was able to substitute the native Hfq functions emphasizing the importance of the conserved N-terminal half of Hfq.[51-52] However, the Woodson lab has recently reported a new role for the C-terminal region of Hfq. Data suggest that this region is not critical for the pairing of sRNAs with their target mRNAs but instead is required for the release of sRNAs and double stranded RNAs (sRNA-mRNA pair) from the Hfq hexamer and hence plays an important role in recycling of the Hfq *in vivo*.[53]

Hfq interacts with proteins and/or protein complexes. As mentioned earlier, Hfq's interaction with 30 proteins or large protein complexes have been experimentally identified. Most of the proteins or partners of protein complexes play important roles in transcription, translation, RNA metabolism and protein folding. The nature of interactions between Hfq and most of these complexes that are either (i) direct, or (ii) indirect via RNA or DNA molecules that have not been well elucidated. A few of the Hfq- protein or protein complex interactions which have been well

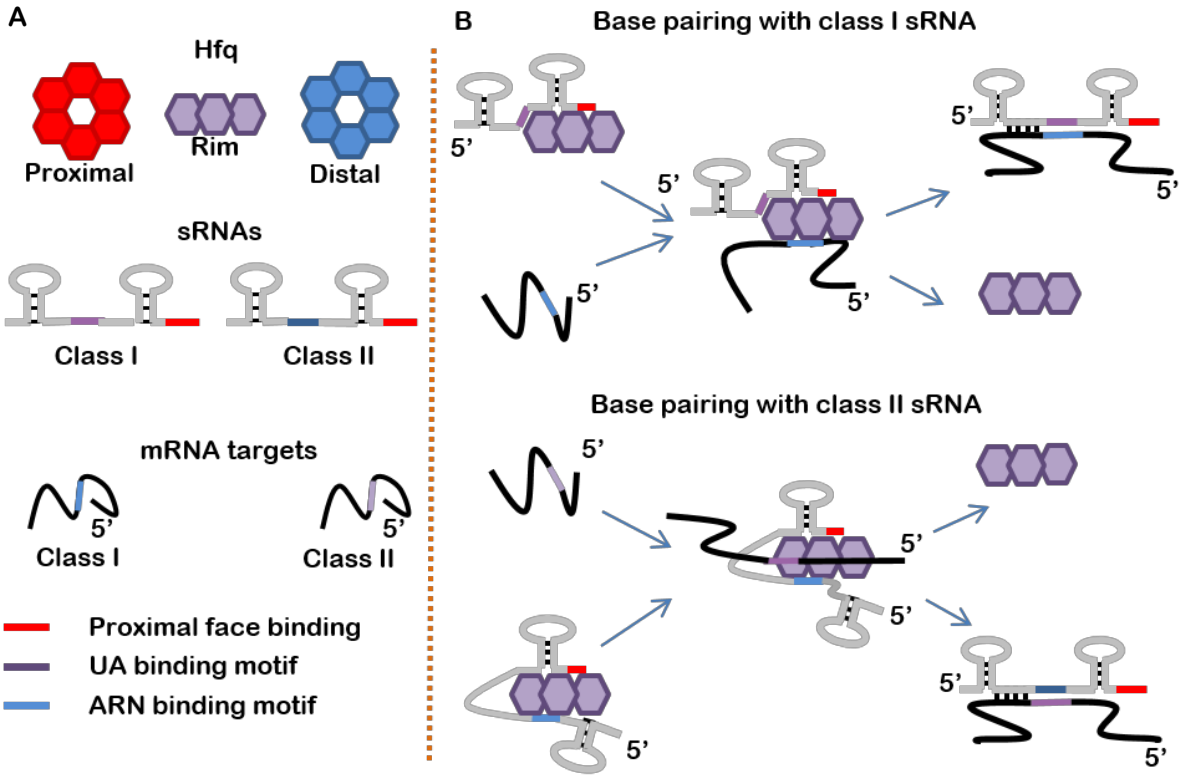

Fig 1.5: Modes of sRNA-mRNA pairing mediated by Hfq. (A) proximal (red), rim (violet) and distal (blue) faces of Hfq hexamers are shown as cartoon pic. Two different class of Hfq binding sRNAs are shown, with Rho independent terminator (proximal face binding) poly U tail (red line) and the rim binding region (violet line) in class I sRNA, and distal face binding region (blue line) in class II sRNA. Two classes of mRNA, class I with ARN binding motif(s) (blue line) and class II with rim binding UA motifs (purple line) are shown as cartoons. (B) Class I sRNA binds to the proximal face of Hfq using proximal face binding motif (red line portion of sRNA) and makes a second contact using the rim binding UA motifs (red line). Class I binds to the Hfq on distal face using ARN motif(s) (blue line portion of mRNA. Formation of sRNA-Hfq-mRNA quartnery structure is followed by the pairing of sRNA with the target mRNA and release of Hfq (shown above the dotted line). Class II sRNA binds to the Hfq on both proximal and distal faces using corresponding binding motifs. Binding of class II mRNA to the Hfq rim results in quartnery structure lead to sRNA-mRNA pairing and release of Hfq. [49]

studied include Hfq interactions with RNaseE, the ribosomal protein S1 and the RNA polymerase (RNAP) complex. [54-58]

1.2.1 Hfq interactions with RNaseE: The RNaseE-Hfq interaction is one of the most prominent example of Hfq's direct interaction with a protein.[59] RNaseE is a ribonucleolytic protein that plays a central role in RNA degradation via the RNA-degradosome in *E. coli.* Under normal conditions, RNA-degradosome is a hetero-multimeric assembly of RNaseE, RhlB (a DEAD-box RNA helicase), enolase and polynucleotide phosphorylase (PNPase).[60] However, the H. Aiba group has shown that the Hfq interaction with RNaseE is independent of the degradosome components and doesn't require RhlB or enolase. Hfq anchors itself on the RNaseE C-terminal scaffold between amino acid residues 702-811 and facilitates the degradation of bound sRNA-mRNA pairs.[56-58] PNPase, which is a part of degradosome, also interacts independently with Hfq and does not need RNaseE mediation.[61] One of the proposed models for Hfq-RNaseE mediated sRNA-mRNA degradation suggests that Hfq binds to the C-terminal scaffold of RNaseE followed by sRNA binding to Hfq.[57] The bound sRNA then searches and pairs up with its target mRNA with the help of Hfq followed by RNaseE mediated ribonucleolytic degradation. sRNA-mRNA-Hfq-RNaseE complex could lead to the degradation of bound RNAs **(Fig 1.6A).**[60, 62] An alternate model suggests the recruitment of RNaseE by the sRNA-Hfq-mRNA ternary complex followed by the degradation of RNAs **(Fig 1.6B)**. Allosteric activation of RNaseE by certain sRNAs has been proposed by Bandyra *et al.*.[63] Their results show that RNaseE activation occurs with Hfq bound sRNA where sRNA carries 5' monophosphate. Upon recognition of the 5' monophosphate of sRNAs, allosteric activation of RNaseE leads to the degradation of mRNA, allowing sRNAs to be released from the truncated mRNAs to recycle the sRNAs **(Fig 1.6C)**.[63]

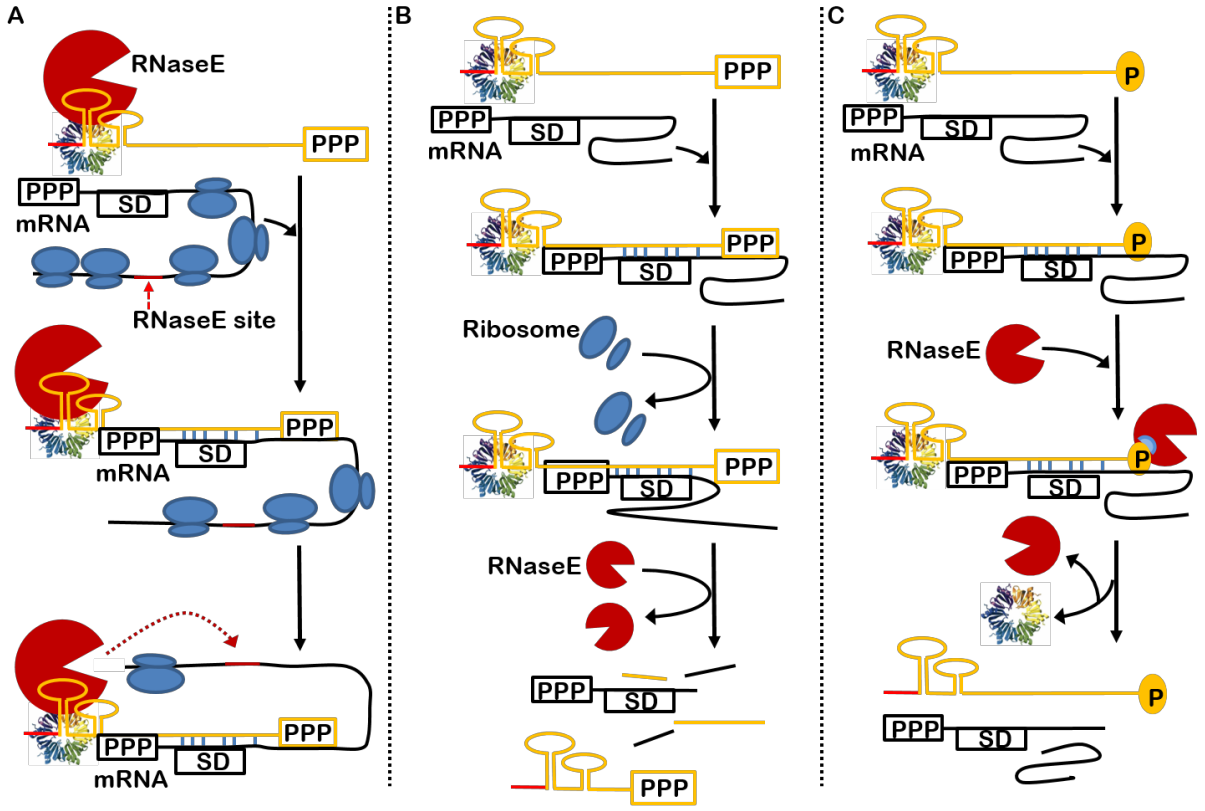

Fig 1.6: Hfq-RNaseE mediated degradation of sRNA-mRNA complex. (A) RNaseE binds with Hfq followed by sRNA to make the ternary complex. sRNA finds the target mRNA and leads to the target degradation at RNaseE site, which could be near or distant to the RNaseE-Hfq-sRNA anchoring site on target mRNA. (B) RNaseE recruitment by sRNA-Hfq-mRNA ternary complex followed by the rapid degradation of RNAs (C) Binding of 5' monophosphate of sRNA to the RNaseE leads to the allosteric activation of RNaseE. RNaseE then cuts the mRNA and allow the release of sRNA; recycling of sRNA. [60, 62,63]

1.2.2 Hfq forms a protein complex with ribosomal protein S1 and RNA polymerase (RNAP): Ribosomal protein S1 and the RNAP beta-subunits have been pulled down along with Hfq from *E. coli* extract when different sRNA baits (DsrA, MicF, OxyS, RyhB or Spot42) were used.[54] However, recombinantly expressed Hfq shows little to no interactions *in vitro* with the RNAP core region and S1 protein separately, which might be indicative of some RNA acting as a common platform for all three proteins.[55] Another pull down assay, which used Hfq as bait and *E. coli* extracts treated with nuclease, revealed the presence of both S1 protein and RNAP subunits in the protein complex, indicating that these proteins might interact together at the interface to form larger protein complexes.[34]

1.2.3 Hfq interaction with Rho inhibits transcription termination: In a recent study Rabhi *et al.*, showed that Hfq interacts with the transcription termination factor Rho and forms a stable binary complex in vitro. Hfq interaction with Rho inhibits the helicase and ATPase activities of Rho to impedes the Rho-dependent transcription termination.[64] However the affects of Hfq mediated Rho antitermination on gene regulation is not well understood.

1.2.4 Catabolite regulator Crc interacts with Hfq to form a co-complex: Crc is a global regulator and plays an important role in the catabolite repression and optimization of metabolism in *Pseudomonas* under nutrient constrained situations. Inactivation of the *Crc* gene results in the altered expressions of at least 134 genes in *Pseudomonas putida*, as verified by transcriptomic and proteomic analyses.[65] Most of the altered genes are involved in sugar and amino acid uptake and assimilation. Under limiting nutrient condition Crc modifies the expression of different transport proteins responsible for amino acid uptake by selectively downregulating some transporter genes in comparison to others.[66-67] Crc is known to bind to an AAnAAnAA motif (where 'A' is Adenine and 'n' could be any nucleotide in a transcript; AAnAAnAA motif is also known as catabolite

activity motif) present in the mRNA, and inhibits translation. Hence Crc also acts as a posttranscriptional regulator.[68-70] An *in vitro* study has shown that Crc itself does not bind to the AAnAAnAA; however it binds to this motif in the presence of Hfq, forming a co-complex. Inactivation of either *crc* or *hfq* results in impaired catabolite repression to similar extents. Thus, it has been proposed that Crc and Hfq come together and form a co-complex with the AAnAAnAA motif to inhibit translation initiation.[71-72]

1.2.5 RelA promotes Hfq multimerzation: RelA synthesizes the (p)ppGpp molecules as a part of a stringent response under amino acid starvation condition in *E. coli*. It is a ribosome associated (p)ppGpp synthetase that, when activated, synthesizes (p)ppGpp molecules, the accumulation of which inhibit rRNA and tRNA synthesis.[73-76] A recent study has shown that RelA promotes the multimerization of Hfq and stimulates Hfq binding to sRNA RyhB.[77]

1.2.6 YbeY also modulates Hfq dependent sRNA expression: YbeY RNase is a single strand-specific endonuclease. It plays an important role in 16s rRNA maturation as well as rRNA promoter transcription antitermination. Deletion of *ybeY* causes defective ribosomal activity and assembly and translational infidelity.[78-80] A *ybeY* deficient *E. coli* strain is temperature sensitive and has a reduced ability to recover from high temperature stress.[81] YbeY also plays a determining role in how *E. coli* responds to hydroxyurea. It was suggested that YbeY can also interact with sRNAs and might contribute to sRNA mediated gene regulation in an Hfq dependent and/or independent manner.[82] Differential expression of twenty-eight sRNAs were observed when Δ*ybey* and *wt E. coli* were exposed to hydroxyurea. Out of 28 YebY dependent sRNAs, 12 sRNAs including the widely studied OxyS, DsrA, and SgrS, are Hfq dependent, whereas other 16 sRNAs **(Table. 1)** were found to be Hfq independent.[83] Further investigations to validate the mechanisms

by which YbeY regulates sRNA-mRNA interactions and the direct or indirect involvement of Hfq would augment our understanding.

	Hfq dependent	Hfq independent
sRNAs binding to YbeY	OxyS, DsrA, CyaR, ArcZ, RybB, MicA, GlmZ, RyeA, RyeB, CydC, RyjB, SgrSs.	Ffs, RygD, CsrC, RdlD, RdlA, GadY, PsrD, RygC, RyfD, RyfA, RybA, RyrC, RyeD, RydB, IsrB, IsrC.

Table 1: sRNAs whose expression where altered in *ΔybeY* strain. Both Hfq dependent (12/28) and independent RNAs (16/28) were found with altered expression.

1.3. ProQ-sRNA interaction: ProQ is a newly declared global post-transcriptional regulator with the capacity to bind and mediate sRNAs' expression and regulatory functions in *Salmonella*. ProQ has been reported to affect the expression of osmoregulatory protein ProP by a mechanism which is not yet understood well.[84] ProQ also has a separate N-terminal domain which resembles the RNA binding protein FinO, and a C-terminal domain which resembles Hfq.[84-86] Studies using the individual domains of ProQ have also shown that the N-terminal domain of ProQ can form strong interactions with RNA, while the C-terminal domain can perform RNA duplexing and strand exchange.[84] A recent study, where an attempt was made to classify RNAs as per their cognate RNA binding protein partner(s), identified ProQ as a global transcriptional regulator. ProQ binds to about 100 RNAs identified by a co-immunoprecipitation study, which include sRNAs, transcription attenuators, and RNAs which act as sponges for sRNAs. The binding affinity of ProQ to sRNAs is high and very similar to Hfq and CsrA. One striking difference is that ProQ binds to highly structured sRNAs whereas Hfq and CsrA bind to single stranded region of sRNAs. ProQ deletion affected expression of >800 transcripts and the expression of ProQ binding sRNAs modulated in a ProQ dependent manner.[36-37, 87]

1.4. CsrA-sRNA interaction: CsrA is a carbohydrate metabolism regulator that affects glycolysis, gluconeogenesis, glycogen degradation and glycogen biosynthesis. Apart from that, CsrA is also

involved in regulation of bacterial motility and biofilm formation among many genes. Active CsrA is present as a homodimer. CsrA is an activator of its own inhibitor sRNA CsrB.[88-89] CsrA binds specifically to the GGA ribonucleotide motif present in multiple hairpin loop structures of the transcript CsrB. CsrA binds to CsrB in an unusually high stoichiometric ratio of 18:1.[90-91] Therefore, CsrA is effectively sequestered by the CsrB, making it unavailable to bind for the CsrA regulated transcripts and hence up or down-regulating the target genes. Besides binding to CsrB, CsrA binds to another sRNA McaS, which is a validated Hfq-dependent regulatory sRNA. CsrA binds to McaS in stoichiometric ratio of 2:1.[92] A bioinformatics study investigating CsrA binding to sRNAs used the presence of AGGA/ARGGA motif as one of the criteria to identify its sRNA partners, after having successfully found the known sRNA partners, they predicted several other possible partners of CsrA in the many bacterial species. [93] A recent study has shown that CsrA binds to the consensus sequence ANGGA when present in hairpin loops in the target transcripts.[35]

1.5. Investigating other protein partners of Hfq-sRNAs mediated gene regulation

Besides the above-mentioned proteins, there might be other proteins which contribute to sRNA mediated gene regulation in an Hfq dependent or independent manner. To identify such proteins, Dr. Lee performed an Hfq-ribonucleoprotein (Hfq-RNP) pull down assay using three known Hfq binding sRNAs RydB, DsrA and SgrS, separately as baits. After orthogonal purification, the Hfq-RNP complexes obtained were analyzed by LC-MS and MALDI-TOF and several protein partners were identified, which may or may not directly interact with Hfq **(Fig 1.7).** As expected many known RNA binding proteins were identified in all three RNP complexes. However, few proteins were present only in specific RNP complexes. Among several proteins which appeared in specific RNP complexes RhlB and RhlE are particularly very interesting. RhlB appeared in an RNP

complex when RydB sRNA was used as bait. RhlE appeared twice, in complexes pulled down using SgrS and DsrA sRNAs. RhlB and RhlE are among the five DEAD box helicases found in *E.*

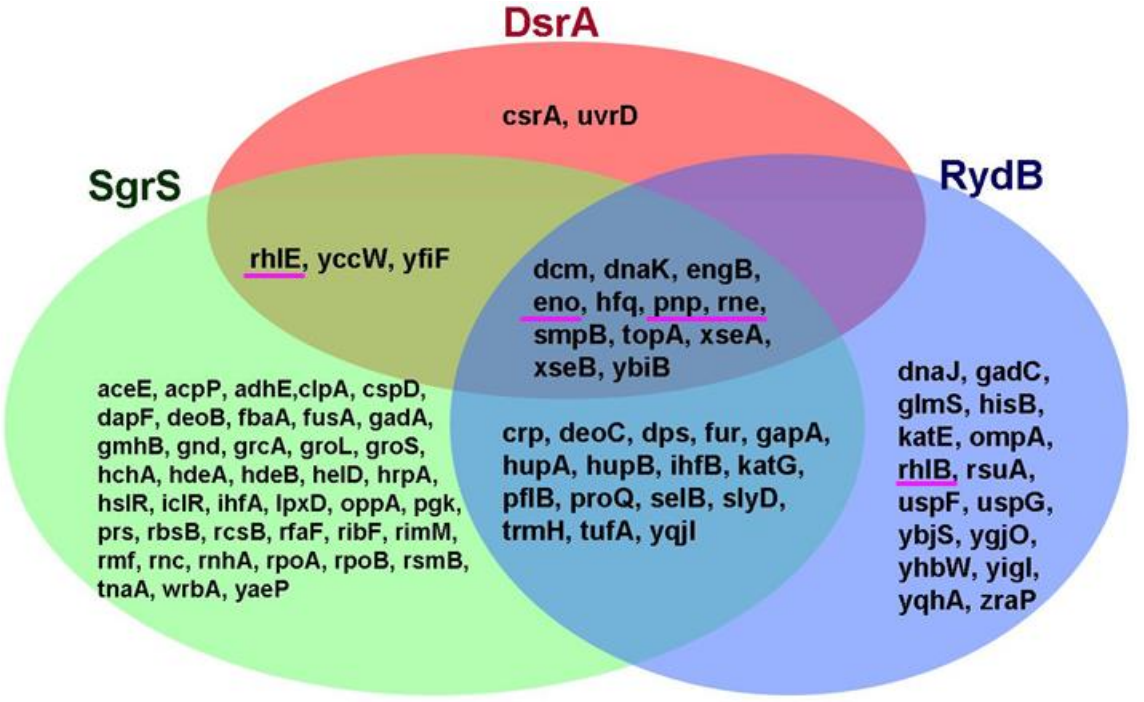

Fig 1.7: Proteins identified from the Hfq-RNP complex pulled down experiments using different sRNAs as bait. Proteins specific to RNP complexes and present in multiple RNP-complexes are shown using a Venn diagram. Underlined proteins are part of the RNA degradosome, RhlB and RhlE are underlined as were identified in RydB-Hfq-RNP complex and DsrA/SgrS-Hfq-RNP complexes respectively.

coli. Under normal conditions RhlB is the helicase partner of the *E. coli* RNA degradosome, the machinery responsible for rapid clearance of transcripts in RNaseE dependent manner. RNP pull down results showed the presence of RNaseE, enolase and PNPase in all three RNP complexes as expected. But, RhlB appearing only in one RNP complex and was replaced by RhlE in other two RNP complexes was an interesting find. Results from Dr. Lee's RNP pull down assays and the information available on DEAD-box helicases led us to hypothesize that **specific DEAD box helicase can be recruited by the sRNA-Hfq complexes under certain conditions to assist in their regulatory functions**.

Discussion on DEAD box helicases and my work related to RhlB and RhlE and their possible roles in sRNA-Hfq mediated gene regulation are presented in chapter 2.

Chapter 2: Stimulation of DEAD-box helicase RhlB and RhlE by sRNA and mRNA of Hfq-mediated gene regulatory pathways.

2.1 DEAD-box RNA helicase: the omnipresent partners of RNA metabolism

DEAD-box RNA helicases are the largest class of RNA helicases and have nine conserved motifs including Asp-Glu-Ala-Asp (D-E-A-D), from which the name DEAD-box helicases has been derived.[94] DEAD-box RNA helicases are associated with pre-mRNA splicing, mRNA turnover, translation initiation and termination, RNA transport, and ribosome biogenesis.[95–98] These proteins are present in all three domains of life. DEAD-box helicases play central and, in many cases essential physiological roles in RNA metabolism.[98–101] The number of DEAD-box RNA helicases varies depending on the organism and can range from as few as 5, as with *E. coli*, to as many as 27 in *Saccharomyces cerevisiae* or 37 in humans.[102–104] Despite being the largest class of RNA helicase proteins, DEAD-box proteins have poor helicase activity and are less processive than other helicases when acting on long RNA duplexes.[105–107]

DEAD-box proteins are ATP driven motors that can unwind or anneal the RNA strands. These enzymes can also restructure and refold a misfolded RNA. The D-E-A-D motif has been found to be important for the ATPase and the RNA unwinding activity exhibited by DEAD-box helicases. The role of ATP in unwinding and translocation of the double stranded RNA by these helicases is not very clear. However, ATP is required for the recycling of the enzyme. Hence, the ATP hydrolysis by DEAD-box helicases is not a direct requirement of strand displacement or unwinding activities. However, the binding of the enzyme to the RNA substrate stimulates the ATPase activity of these helicases.[108] DEAD-box helicases can bind to their specific RNA targets to perform specialized functions. Figure 2.1 depicts the different modes of substrate targeting used by DEAD-box helicases that have been previously identified[109] including: (A) the specific

recognition of an RNA hairpin loop by the helicase core, which occurs during the binding of

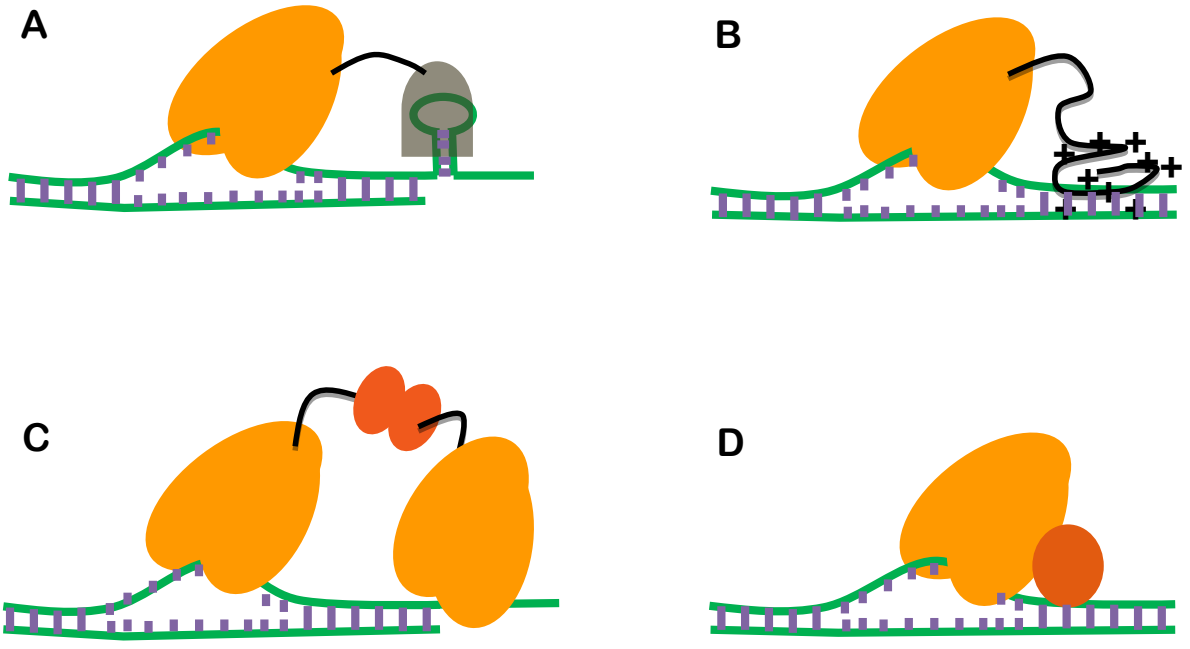

Figure 2.1. Modes of substrate recognition and binding of DEAD-box helicases.[109] **(A)** Recognition of specific RNA hairpin loop structure by DEAD-box helicases;[110-113] **(B)** Nonspecific binding of structured RNAs mediated by C-terminal basic tail regions of DEAD helicases;[114,115] **(C)** Nonspecific targeting by multimerization of helicases allowing to form multiple interactions with structured RNA substrate;[116] **(D)** Targeting the RNA substrate through protein-protein interaction of helicase core with accessory proteins.[117]

hairpin 92 in the 23S rRNA and DbpA by the YxiN DEAD-box helicases;[1110-113] (B) Nonspecific binding of structured RNAs mediated by C-terminal basic tail regions possessed by DEAD-box helicases as with SrmB, Mss116p, and Ded1p;[114,115] (C) Nonspecific targeting by multimerization of helicases allowing multiple interactions with structured RNA substrates; example: the interactions of the dimerization domain of Hera;[116] and (D) Targeting the RNA substrate by protein-protein interaction of helicase core with specific proteins as in the case of helicase Dbp5p.[117] A recent study suggests that the binding of DbpA is region specific and DbpA binds to hairpin 92 using its C-terminal RNA binding domain. Once anchored to helix 92, the catalytic core of DbpA can unwind any nearby double helix. Although, not completed understood, many

examples of similar interactions between DEAD-box helicases and specific proteins have found suggesting that DEAD-box proteins may be involved in many cellular functions and pathways.[118]

E. coli has five DEAD-box helicases (CsdA, DbpA, RhlB, RhlE and SrmB), which have been associated with ribosome biogenesis and mRNA turnover.[104] Studies suggest that the *E.* coli strains lacking one or more helicases do not exhibit adverse growth defects under normal conditions. Experiments have demonstrated that *E. coli* can grow and survive even with the successful deletion of all five DEAD-box helicases. This suggests that, despite their abilities to anneal, unwind and restructure RNAs, DEAD-box helicases are dispensable in *E. coli*. However, under alternative growth conditions, defects in ribosome and growth in DEAD-box helicase deficient strains become more pronounced.[119-120]

Results from our lab (**Figure 2.1)**, where RhlB and RhlE selectively appeared in different RNP-complexes indicate that there might be a possibility of RhlB and RhlE being recruited by Hfq or the sRNAs to facilitate the sRNA-Hfq mediated gene regulations. Studies from Blasi and co-workers suggested that the regulation of *rpoS* by sRNA DsrA requires CsdA at cold temperatures (15 °C). Hfq fails to facilitate the regulation of *rpoS* by sRNA DsrA on its own, unlike during normal growth conditions, supporting the idea that Hfq or Hfq-sRNA/RNP may recruit DEAD-box helicases under stressful or specific conditions.[121] In this study focuses on the roles of RhlB and RhlE in sRNA mediated regulations and effects of Hfq on RhlB and RhlE.

RhlB is an integral part of the RNA-degradosome machinery in *E. coli*, along with PNPase, enolase and RNaseE.[122-124] RhlB facilitates the PNPase mediated degradation of RNAs with strong secondary structures. The coordination between RhlB and PNPase requires the association of these two proteins with RNase E which acts as a scaffold to anchor all the other components of degradosome. The association of RhlB with the C-terminal end of RNase E (between amino acids

696–762), or a peptide fragment from RNase E (including amino acids 696–762), is known to stimulate the RNA unwinding as well as the ATPase activity of RhlB. The RNA unwinding and ATPase activity further aid the PNPase mediated degradation of structured RNAs.[125-127] However, an RNase E independent RhlB-PNPase complex has been reported that can efficiently mediate RNA degradation.[128-129] A recent report suggests that the interaction of the RNase E independent RhlB-PNPase complex is involved in cysteine homeostasis in *E. coli*. Northern blot analyses showed the accumulation of *cysB* transcript that encodes for a transcriptional activator of the *cys* operon. Microarray analyses showed the upregulation of 11 out of 14 cysteine biogenesis genes validating the high cellular level of cysteine and enhanced antioxidative response.[129] *In vitro*, RhlB shows poor 5'→3' RNA helicase activity while requiring a 5' overhang and fails to unwind blunt end RNA duplexes.[130] RhlB shows stimulated ATPase activity in the presence of an RNA substrate which increases with addition of RNase E peptide fragment (including amino acids 696–792). However, this increased activity is 6–7 fold less than the ATPase activity shown by RhlE and SrmB when total RNA extract from *S. cerevisiae* was used as susbstrate.[125] The low ATPase activity could be because: (a) RhlB has inherently slow ATPase activity; or (b) RhlB is only stimulated by a very specific substrate that could be either less abundant or less available to RhlB due to the competition between RhlB specific and nonspecific substrate RNAs present in the total RNA extract. However, any RNA sequence or region specific binding or stimulation of RhlB's ATPase activity has not been previously reported.

RhlE on the other hand, can unwind dsRNA with 5' or 3' overhangs and RNA duplexes with blunt ends. Unwinding of blunt RNA duplexes is an ability unique to RhlE among the five DEAD-box helicases of *E. coli.*[104,131] RhlE has exhibited higher ATPases activity than RhlB, and to the similar ATPase activity to SrmB when a total RNA extract of *S. cerevisiae* was used as RNA

substrate.[125] Bizebard *et al*. have previously used multiple RNA oligomers to study stimulation of ATPase activity of RhlE, SrmB, CsdA and a CsdA mutant (ΔCsdA). RNA oligomers were used in a high concentration to obtain maximal stimulation. Results have shown that stimulation of DEAD-box helicases occur in a substrate dependent manner. SrmB demonstrates the least stimulation, while the CsdA and ΔCsdA showed moderate stimulation. RhlE exhibits the highest stimulation of the four helicases in the study using data from the same substrate.[131] Results from this study, using specific RNA oligomers, are inconsistent to the results obtained using whole RNA extract of *S. cerevisiae*, where SrmB and RhlE have shown similar activities.[125,131] One possible explanation for the observations from both the studies could be that RhlE is less specific and therefore shows near maximal stimulation under both experimental conditions. However, stimulation of SrmB occurred only when total RNA extract was used. The RNA oligos used by Bizebard *et al*. might not be the optimal substrates for SrmB, emphasizing the fact that DEAD-box helicases might have a sequence or structural preference while binding to their substrate.

RhlE can partially alleviate the effects of the *ΔcsdA* mutation when overexpressed but exacerbates the *ΔsrmB* related phenotypes under cold stress. It has been proposed that RhlE aids SrmB and CsdA in ribosome biogenesis by acting on 50S subunit of the ribosome. The higher RhlE concentration favors the ribosome biogenesis via SrmB mediated pathway instead of the CsdA mediated pathway.[119-120]

Like RhlB, RhlE also anchors to RNase E and binds to a site different binding site than RhlB.[132] In the gram negative bacteria, *Pseudomonas syringae* Lz4W, it has been observed that under cold stress conditions RhlB gets replaced by RhlE.[133] *In vitro* studies demonstrate that a complex constituted with RNaseE, PNPase and RhlE or CsdA can degrade the structured RNA in PNPase dependent manner, similar to RhlB.[132,134] Iresha's work from our lab has previously shown

that the *ΔrhlE* strain grows as robustly as the wild type *E. coli* strain under normal growth conditions. Also, the *ΔrhlE* strain does not show any growth defects when exposed to cold shock, osmotic stress, sugar stress or oxidative stress conditions. However, the *ΔrhlE Δhfq* strain shows a growth pattern like *Δhfq* strain under cold shock and osmotic stress conditions. Normal growth is partially restored in the *ΔrhlE Δhfq* strain compared to the impaired growth normally exhibited by the *Δhfq* strain under sugar stress condition. Furthermore, in the *ΔrhlE Δhfq* strain normal growth is completely restored compared to the *Δhfq* strain under oxidative stress conditions. Considering all these data, it was hypothesized that RhlB and RhlE work synergistically with Hfq to modulate sRNA-mediated gene regulations.

2.2 Investigating the roles of RhlB and RhlE in Hfq-sRNA mediated gene regulation in *E. coli*: approach, results, and discussion

The goal of these experiments was to understand the roles of RhlB and RhlE in Hfq-sRNA mediated gene regulations during the response to stress. We hypothesized that Hfq and RhlB or RhlE can work synergistically or complementarily to modulate the gene regulation. To address this question, a multi-pronged approach was designed.

First the *in vitro* approach has the advantage of the ATPase activity of DEAD-box helicases. Since, DEAD-box helicases are stimulated upon binding to an RNA substrate the hydrolysis of ATP by RhlB or RhlE can be measured using lactate dehydrogenase-pyruvate kinase coupled enzyme assay. The rate of ATP consumption by RhlB or RhlE can be calculated by measuring the decrease in concentration of NADH which absorbs distinctly at wavelength 340 nm **(Figure 2.2)**. We hypothesized that RhlB and RhlE would have differential stimulation with different RNAs because of their preferential binding to certain structural or sequence motifs

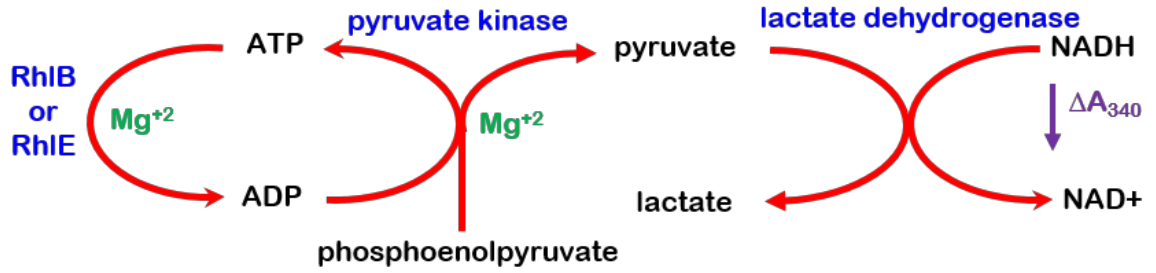

Figure 2.2. Schematics of the coupled enzyme assay. RhlB or RhlE in presence of Mg^{+2} and an appropriate RNA substrate show stimulated ATPase activity, converting the ATP into ADP. Pyruvate kinase converts phosphoenolpyruvate to pyruvate regenerating ATP from ADP in the process. The pyruvate is converted to lactate by lactate dehydrogenase oxidizing NADH to NAD+. NADH absorbs light at 340 nm (Molar extinction coefficient = 6220 L mol^{-1} cm^{-1}) and with the decrease in concentration of NADH, the absorbance at λ_{340} decreases as measured spectrophotometrically. The ATP:NADH consumption ratio is 1:1 therefore the rate of NADH consumption indirectly gives the rate of ATP consumption by the enzyme of interest(RhlB or RhlE).

present in substrates. To understand the differential affinity and stimulation of RhlB and RhlE a variety of RNA substrates were chosen.

RNAs substrate for RhlB and RhlE	**Description of RNA substrates**
rA18	poly-A tails are posttranscriptional modification to mRNA; binds to Hfq.
fhlA53	–53 upstream to AUG of *fhlA* +60
fhlA220	–220 upstream to AUG of *fhlA* to +60
rpoS	–134 upstream to AUG of *rpoS* to +3
ompC	–81 to 60
ompF	–110 to 60
sdhC	–220 to 60
hns	–30 to 60
glmS	–143 to 60
OxyS	Full length
DsrA	Full length
GlmZ	Full length
GlmY	Full length
RyhB	Full length
RybB	Full length

Table 2.1. List of RNAs used to test the ATPase activity of RhlB and RHlE in presence and absence of Hfq. All RNA substrates were prepared by *in vitro* transcription using T7 RNAP except rA18 which was purchased from Dharmacon Research.

Several Hfq dependent sRNAs and their target mRNAs were selected as substrates to study the stimulation of ATPase activity of RhlB and RhlE **(Table 2.1)**. Plasmid constructs with sequences from fhlA53, fhlA220, rpoS, OxyS and DsrA were available from previous studies in the Feig laboratory and the rA18 RNA oligos were purchased from Dharmacon. DNA sequences for the final nine RNA constructs were cloned into pUC19 using the restrictions sites as described in Table 2.3. A T7 RNA polymerase promoter sequence was incorporated into the plasmid for *in vitro* transcription. All sequences were constructed using PCR with a TOP-10 *E. coli* strain

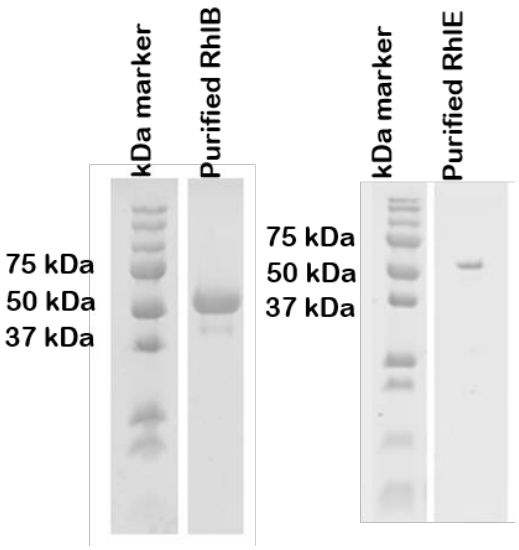

Fig 2.3: Gel analysis of purified RhlB and RhlE. RhlB was purified by Ni^{+2} affinity chromatography and the eluted fraction is loaded on the SDS-PAGE gel (4% stalking, 15% PAGE separation gel). RhlE was purified as mentioned in materials and methods section, and the elution fraction after 2nd Ni+2 affinity column was collected as final purified protein, shown here.

template using Taq DNA polymerase and the appropriate primers and conditions (Table 2.3, Materials and Methods). The identity of each clone was verified by sequencing. *In vitro* transcription experiments were performed using the corresponding linearized plasmids and the RNA products were gel purified. RhlE and RhlB were purified before SDS-PAGE analysis for protein purity **(Figure 2.3)**.

Hfq dependent sRNAs and their partner mRNAs but not the rA18 oligomers stimulated RhlB **(Figure 2.4)**. Coupled enzyme assays were performed using 50 nM of RhlB and 200 nM of RNA substrates to investigate the differential stimulation, if any, while using different RNA substrates. RhlB was stimulated by most of the sRNAs and mRNAs used as substrates but no stimulation was observed with rA18 substrate in the absence of Hfq. However, these ATPase assays were done in absence of RNase E or RNase E peptide fragments (696–762 amino acids) and substrate dependent stimulation of RhlB was observed. Stimulations of RhlB with the RNAs

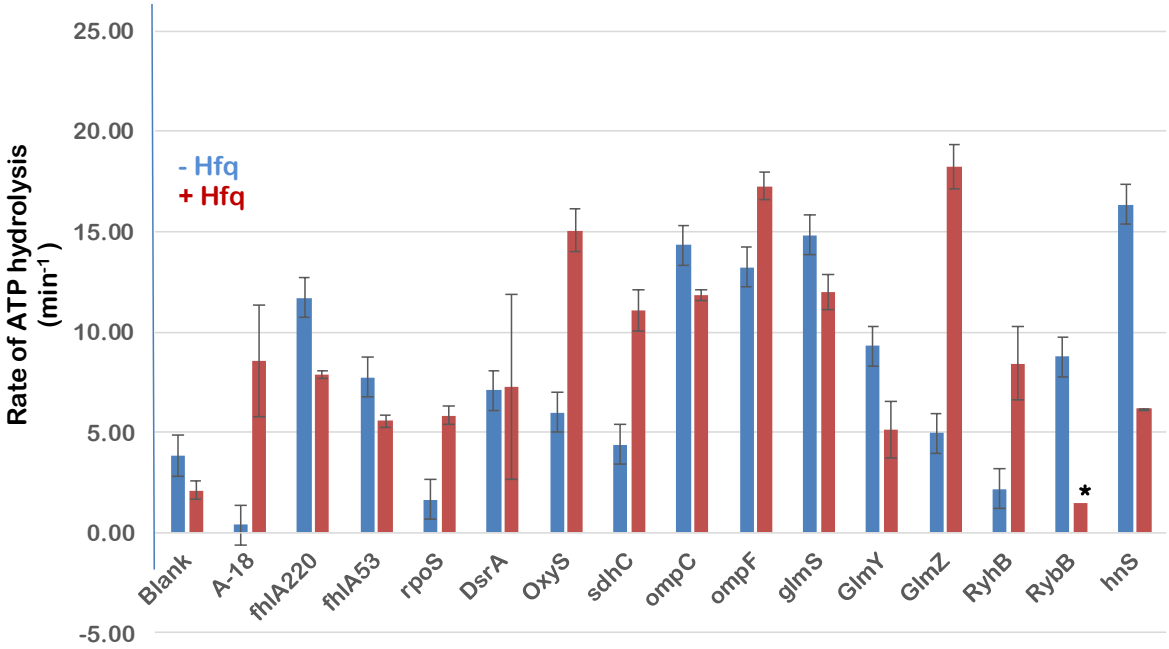

Figure 2.4. RhlB ATPase activity to identify the RNA dependent stimulation. Lactate dehydrogenase-Pyruvate kinase coupled enzyme assay was used to track the progress of reaction. Rate of reaction (ATP hydrolysis) was measured indirectly by measuring the decrease in concentration of NADH at λ_{340}, over the course of 10.0 min reaction time. The measurements were taken at every 30.0 s. Results were analyzed using Microsoft excel. 50.0 nM of RhlB, and 200.0 nM of each RNA substrate was used. The results plotted here are the mean of the results from two independent sets of experiments. Average deviation has been used as error bar. To assess the effect of Hfq, 100nM was used. The number on X-axis indicate the number of moles of ATP hydrolyzed per mole of RhlE, per minute.Data is given in table 2.2.

* RybB data for +Hfq reaction is the data obtained from one set of experiment hence there is no error bar indicated.

used for this study are multiple fold higher than reported by Worrall *et al.*[125] This could be because of the difference in substrates used between these two experiments. It is important to mention that

in my work RhlB has been tested in lower concentrations of substrate. Therefore, the numbers here, most likely, do not represent the maximum stimulation of RhlB by any substrate.

	50.0nM RhlB + 200.0 nM RNAs			25.0nM RhlE + 200.0 nM RNAs		
RNAs	**avg rate (–Hfq)**	**avg rate (+Hfq; 100.0 nM)**	**fold change (+Hfq/–Hfq)**	**avg rate (–Hfq)**	**avg rate (+Hfq; 100.0 nM)**	**fold change (+Hfq/–Hfq)**
Blank	3.8 ± 0.7	2.1 ± 0.5	0.55	7.4 ± 0.0	15.6 ± 6.0	2.12
A-18	0.4 ± 0.2	8.6 ± 2.8	22.15	92.7 ± 23.7	40.5 ± 8.4	0.44
fhlA220	11.7 ± 2.9	7.9 ± 0.2	0.67	190.3 ± 29.1	209.9 ± 18.2	1.10
fhlA53	7.7 ± 1.2	5.6 ± 0.3	0.72	291.5 ± 28.0	228.6 ± 3.0	0.78
rpoS	1.6 ± 0.1	5.8 ± 0.5	3.56	149.4 ± 10.1	170.0 ± 1.5	1.14
DsrA	7.1 ± 0.4	7.3 ± 4.6	1.03	320 ± 15.5	328.3 ± 23.1	1.02
OxyS	6.0 ± 0.3	15.1 ± 1.1	2.52	167.9 ± 16.6	146.6 ± 9.2	0.87
sdhC	4.4 ± 1.4	11.1 ± 1.0	2.52	205.1 ± 5.5	134.8 ± 39.4	0.66
ompC	14.3 ± 0.3	11.9 ± 0.3	0.83	197.2 ± 12.7	139.6 ± 21.4	0.71
ompF	13.2 ± 0.6	17.3 ± 0.7	1.30	188.2 ± 19.5	126.0 ± 14.0	0.67
glmS	14.8 ± 0.8	12.0 ± 0.9	0.81	181.7 ± 1.2	162.1 ± 1.1	0.86
GlmY	9.3 ± 1.5	5.1 ± 1.4	0.55	119.4 ± 10.6	108.2 ± 7.5	0.91
GlmZ	4.9 ± 0.2	18.2 ± 1.1	3.69	133.8 ± 1.4	110.2 ± 2.3	0.82
RyhB	2.2 ± 1.0	8.4 ± 1.8	3.87	332.7 ± 37.9	229.2 ± 9.0	0.69
RybB	8.8 ± 0.5	1.40*	0.16	481.6 ± 70.5	347.3 ± 13.1	0.72
hnS	16.4 ± 0.8	6.2 ± 0.0	0.38	240.3 15.0	174.0 ± 24.0	0.72

Table 2.2: RNA stimulated RhlB/RhlE ATPase activity data. The results given here are the mean of the results from two independent sets of experiments. Average deviation has been used as error bar (±). To assess the effect of Hfq, 100 nM was used as indicated. The numbers indicate the number of moles of ATP hydrolyzed per mole of helicase (RhlB or RhlE), per minute; in presence of 200.0 nM of corresponding RNA substrate.

*RybB data for +Hfq reaction is the data obtained from one set of experiment hence there is no error indicated.

In presence of Hfq (100.0 nM), stimulation of RhlB has shown a mixed pattern. As evident from Figure 2.3 and Table 2.2 presence of Hfq resulted in higher stimulation of RhlB (more than two folds) for rA18, OxyS, RpoS, SdhC, GlmZ and RyhB substrate. Significant decrease (more than two folds) in stimulation occurred only for RybB and Hns. RybB data is from a single experiment and therefore it is hard to draw any conclusions from it. Presence of Hfq has not made any significant difference in ATPase activity of RhlB for rest of the RNA substrates.

RybB caused the strongest stimulation of RhlE's ATPase activity among all the RNA substrates used **(Figure 2.5)**. All RNA substrates caused strong stimulation of ATPase activity however, stimulation by RybB was the strongest followed by RyhB, DsrA and fhlA53. rA18

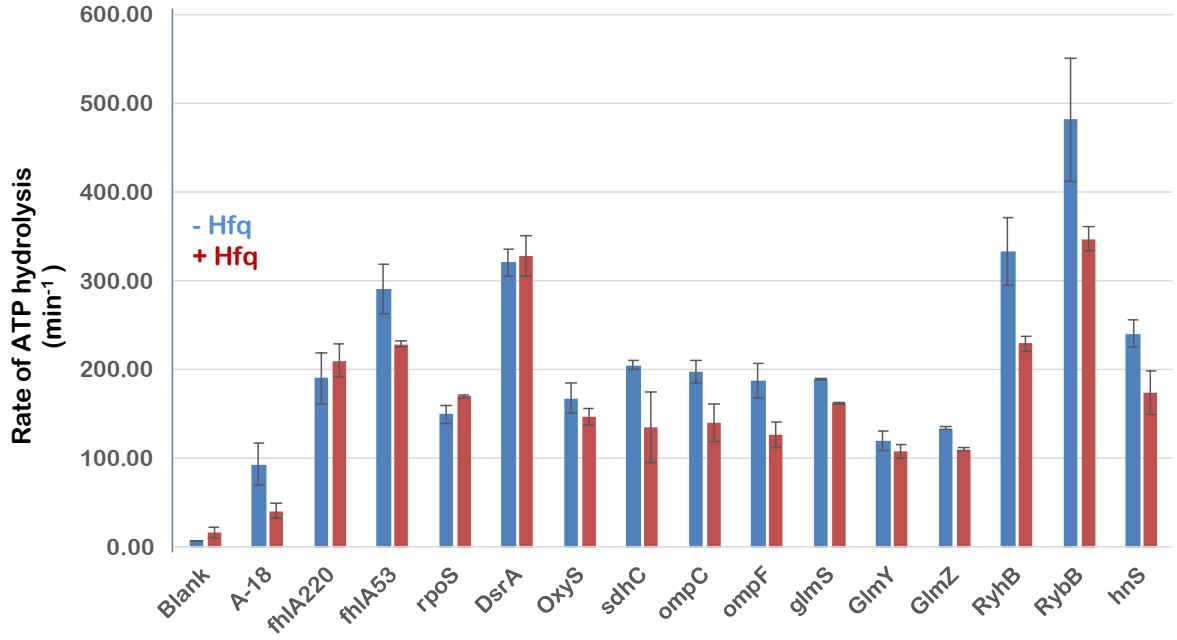

Figure 2.5: RhlE ATPase activity to identify the RNA dependent stimulation. Lactate dehydrogenase-Pyruvate kinase coupled enzyme assay was used to track the progress of reaction. Rate of reaction (ATP hydrolysis) was measured indirectly by measuring the decrease in concentration of NADH at λ_{340}, over the course of 10.0 min reaction time. The measurements were taken at every 30.0s. Results were analyzed using Microsoft excel. 25.0 nM of RhlE, and 200.0 nM of each RNA substrate was used. The results plotted here are the mean of the results from two independent sets of experiments. Average deviation has been used as error bar. To assess the effect of Hfq, 100nM was used. The number on X-axis indicate the number of moles of ATP hydrolyzed per mole of RhlE, per minute. Data is given in table 2.2.

caused the weakest stimulation among all the RNA substrates however, the result is consistent with the literature reported value for rA16 (110 min^{-1}) and rA18 (120 min^{-1}). Again, it is important to note that the RNA substrates used are not in such high concentrations which yields the maximum stimulation. Therefore, the number obtained for stimulation of ATPase in presence of rA18 (92.7 ± 23.7) could be higher if higher concentration of rA18 being used. Presence of Hfq invariably decreased the RNA substrate stimulated rate of ATP hydrolysis.

Presence of Hfq invariably decrease the rate of ATPase stimulation in case of RhlE, whereas it displays entirely different behavior with RhlB. To explain the effects of Hfq on RhlB and RhlE, we offer few possibilities and explanation to their outcomes. (a) RhlB and RhlE binds to the RNA at the same site as Hfq: this could lead to the competition between two proteins or sequestration of free RNA substrates by Hfq, and hence the decrease in ATPase activity would be observed. (b) RhlB and RhlE binds to the RNA substrate at an entirely different site than Hfq without causing any change to the RNA structure. Therefore, presence of Hfq would not have a big impact on ATPase activity of helicases. The binding sites for the two proteins would be distinctly available except, when the two sites are too close and cause steric hindrance or assists other protein to bind to the substrate (cooperative binding of protein). In that case, ATPase activity could either decrease or increase, respectively. (c) Binding of Hfq results in remodeling of RNA substrate and could (i) expose, (ii) seclude, or (iii) show no effect at the helicase binding sites. Depending on the outcome of Hfq mediated remodeling the ATPase activity could increase, decrease or remain unaffected. Nonetheless, this data presented raised a few interesting questions.

(a) Does RhlB prefer a structural or sequence element during the substrate selection?
(b) Does RhlB require assistance of Hfq, *in vivo*, to accomplice its function as a component of RNA degradosome under normal or certain stress conditions?

It is tempting to speculate that RhlB which acts as regular component of RNA could use assistance of Hfq, under certain conditions. However, higher processive RhlE might not need Hfq assistance to perform its function.

To study the roles of RhlB and RhlE, *in vivo*, *ΔrhlB, ΔrhlB Δhfq, ΔrhlB ΔrhlE, and ΔrhlB ΔrhlE Δhfq* were prepared (data not shown). The *ΔrhlE, ΔrhlE Δhfq* strains were prepared by our previous lab member Iresha Rahnayake. The goal was to use these strains to understand the effect of the

deletion of *rhlB, rhlE and hfq* on growth, by exposing the *E. coli* strains to different stress conditions. Due to certain constrains the *in vivo* studies could not be done.

So far, this study has shown that RhlB and RhlE get significantly stimulated with the Hfq binding sRNAs and mRNAs. Further, investigations would be required to understand the effects of Hfq on RhlB activities. Understanding the contribution of RhlB and RhlE to sRNA-Hfq-mediated gene regulation would enrich our knowledge of regulatory pathways, and help eradicate the pathogenic bacteria.

Chapter 2: Materials and methods

Cloning of RhlB: *rhlB* was PCR amplified using Taq-DNA polymerase (1X $MgCl_2$-free Taq DNA polymerase buffer, 0.5 mM $MgCl_2$, 0.8 mM dNTPs mix, 0.2 µM each primer and 5.0 µL of boiled Top-10 *E.coli* cells). *rhlB* forw and *rhlB* rev primers were and corresponding temperature profile as mentioned in table 2.3. PCR reaction was analyzed using 1.2 % Agarose gel, visualized using ethidium bromide. The identified PCR product was cleaned up using PCR clean up kit (E.Z.N.A. Microelute cycle-Pure Kit; Omega, D6293-03). pET28a vector (2.0 µg) and the PCR product (2.0 µg) were separately digested with NcoI and HindIII in 50.0 µL reaction size. Digested PCR product and vector were cleaned again using PCR clean up kit same as mentioned before. Cleaned PCR product was then inserted into pET28a vector using T4-DNA ligase (NEB, M0202S) following the manufacturer's protocol. The ligation mixture was then transformed into Top-10 *E. coli* stain and plated on LB-Agar plate containing 30.0 mg/ml Kanamycin. Single colonies were analyzed for the presence of correct *rhlB* carrying pET28a plasmids using pET28a specific primers. Plasmid minipreps were done using E.Z.N.A plasmid DNA Mini Kit II (Omega, D6945-02) and purified plasmids were used for restriction digestion to re-confirm the presence of *rhlB* in the purifies plasmid. Plasmids identified positive for the *rhlB* were then sequenced using pET28a specific sequencing primers as well *rhlB* internal reverse and forward primers. Selected plasmid was then transformed into the BL21(DE3) cells for expression purpose. Transformation of plasmids were done in our lab prepared electrocompetent cells of Top-10 and BL21(DE3) where needed, using Bio-Rad micropulser.

Expression and purification of RhlB: BL21(DE3) cells were streaked on a LB-Agar-Kanamycin (30 mg/ml) plate. 5.0 ml LB-media was inoculated with cells picked from the single colony. The overnight culture was then used to inoculate fresh 1 L of LB-media and cells were grown (250 rpm

@ 37 °C), until OD_{600} of 0.4–0.5 have been reached. Cells were induced with IPTG (final concentration of 1mM) to express the protein for 4–5 hours. Cells were harvested (5000 g, 10min @ 4 °C) and cells pellet was stored in @ –20 °C until ready for purification.

Cell pellet was thawed on ice and then suspended into ice cold lysis buffer (25 mM Tris-HCl, 300.0 mM KCl and 10.0 mM imidazole; pH 8.1) up to the volume of 15.0 – 20.0 ml. Half a tablet of proteases inhibitor cocktail (ROCHE, cOmplete from Sigma – 11697498001) was added and the lysis was done by sonication (4–5 cycles of 30s pulse with 1.0 min pause @ 37 % amplitude). Lysed cells suspension was then clarified to obtain the clear supernatant by centrifugation (30,000 rpm for 45 min @ 4 °C, using JA-17 rotor). Clear supernatant was then filtered through 0.8 micron syringe filter and transported to cold room (2 – 6 °C) for further purification. The clear supernatant was loaded on to a charged Ni affinity column pre-equilibrated with lysis buffer. After loading of supernatant, the Ni column was washed with 10 column volume (CV) of lysis buffer followed by 10 CV of imidazole buffer (10 mM HEPES, 300.0 mM KCl and 50.0 mM imidazole; pH 7.5), then 10 CV of high salt buffer (10 mM HEPES, 1.0 M KCl and 10.0 mM imidazole; pH 7.5), before eluting the protein off the column using 10 CV of before elution buffer (10 mM HEPES, 1.0 M KCl and 300.0 mM imidazole; pH 7.5). Elution fraction collected was then used for analyzing the presence of protein using denaturing SDS-PAGE gel (4 % stalking, 15 % separation gel), visualized by Coomassie staining. Eluted fraction then dialyzed twice, using 1 L of dialysis buffer (10 mM HEPES, 300.0 mM KCl; pH 7.5) at 4 °C or in cold room, with gentle spinning. Dialyzed protein was kept on ice and filtered using 0.2 micron syringe filter before determining the concentration of protein using $A_{280/260}$ ratio. Protein is then diluted, if needed, 1.0 – 1.5 mg/ml concentration and stored at 4 °C to be used for coupled enzyme assay for next 15–20 days. Protein older than 15–20 days stored at 4 °C were never used for coupled enzyme assay.

Expression and purification of RhlE: BL21(DE3) cells (prepared previously by Iresha Rathnayake) were streaked on a LB-Agar-Kanamycin (30 mg/ml) plate. 5.0 ml LB-media was inoculated with cells picked from the single colony. The overnight culture was then used to inoculate fresh 1 L of LB-media and cells were grown (250 rpm @ 37 °C), until OD_{600} of 0.4–0.5 have been reached. Cells were induced with IPTG (final concentration of 1mM) to express the protein for 4–5 hours. Cells were harvested (5000 g, 10min @ 4 °C) and cells pellet was stored in @ –20 °C until ready for purification.

Cell pellet was thawed on ice and then suspended into ice cold lysis buffer (25 mM Tris-HCl, 300.0 mM KCl and 10.0 mM imidazole; pH 8.1) up to the volume of 15.0 – 20.0 ml. Half a tablet of proteases inhibitor cocktail (ROCHE, cOmplete from Sigma – 11697498001) was added and the lysis was done by sonication (4–5 cycles of 30s pulse with 1.0 min pause @ 37 % amplitude). Lysed cells suspension was then clarified to obtain the clear supernatant by centrifugation (30,000 rpm for 45 min @ 4 °C, using JA-17 rotor). Clear supernatant was then filtered through 0.8 micron syringe filter and transported to cold room (2 – 6 °C) for further purification. The clear supernatant was loaded on to a charged Ni+2 affinity column pre-equilibrated with lysis buffer. After loading of supernatant, the Ni+2 column was washed with 10 column volume (CV) of lysis buffer followed by 10 CV of imidazole buffer (10 mM HEPES, 300.0 mM KCl and 50.0 mM imidazole; pH 7.5), followed by 10CV Urea buffer (10 mM HEPES, 300.0 mM KCl, 1.0 M Urea and 10.0 mM imidazole; pH 7.5) 10 CV of high salt buffer (10 mM HEPES, 1.0 M KCl and 10.0 mM imidazole; pH 7.5), before eluting the protein off the column using 10 CV of before elution buffer (10 mM HEPES, 1.0 M KCl and 300.0 mM imidazole; pH 7.5). Elution fraction collected was then used for analyzing the presence of protein using denaturing SDS-PAGE gel (4 % stalking, 15 % separation gel), visualized by Coomassie staining.

Eluted fractions were then aliquoted in two 5.0 mL fractions and loaded separately (two separate runs) on to the Superdex S-200 column for size exclusion chromatography using Bio-Rad NGC FPLC system and FPLC-buffer (10 mM HEPES, and 300.0 mM KCl; pH 7.5) for elution. The FPLC fractions containing protein were loaded on 2nd Ni+2 affinity column, charged and pre-equilibrated with FPLC buffer, to concentrate the protein. Protein was then eluted like 1st Ni+2 column without using any wash step. Eluted fractions (~ 10.0 mL) were then filled in to a dialysis cassette (10,000 MW) and dialyzed twice, using 1 L of dialysis buffer (10 mM HEPES, 300.0 mM KCl; pH 7.5) at 4 °C or in cold room, with gentle spinning. Dialyzed protein was kept on ice and filtered using 0.2 micron syringe filter before determining the concentration of protein using $A_{280/260}$ ratio. Protein is then diluted, if needed, 1.0 – 1.5 mg/ml concentration and stored at 4 °C to be used for coupled enzyme assay for next 15–20 days. Protein older than 15–20 days stored at 4 °C were never used for coupled enzyme assay.

Expression and purification of Hfq-CH6-wt2: BL21(DE3) carrying the expression plasmid *Hfq-CH6-wt*2 for cells (from lab stock) were streaked on a LB-Agar-Kanamycin (30 mg/ml) plate. 5.0 ml LB-media was inoculated with cells picked from the single colony. The overnight culture was then used to inoculate fresh 1 L of LB-media and cells were grown (250 rpm @ 37 °C), until OD_{600} of 0.4–0.5 have been reached. Cells were induced with IPTG (final concentration of 1mM) to express the protein for 4–5 hours. Cells were harvested (5000 g, 10min @ 4 °C) and cells pellet was stored in @ -20 °C until ready for purification.

Cell pellet was thawed on ice and then suspended into ice cold lysis buffer (50 mM Tris-HCl, 250.0 mM NH_4Cl, 20.0 mM imidazole and 10 % glycerol; pH 7.5) up to the volume of 15.0 – 20.0 ml. Half a tablet of proteases inhibitor cocktail (ROCHE, cOmplete from Sigma – 11697498001) was added and the lysis was done by sonication (4–5 cycles of 30s pulse with 1.0

min pause @ 37 % amplitude). Lysed cells suspension was then clarified to obtain the clear supernatant by centrifugation (30,000 rpm for 45 min @ 4 °C, using JA-17 rotor). Clear supernatant was then filtered through 0.8 micron syringe filter and transported to cold room (2 – 6 °C) for further purification. The clear supernatant was loaded on to a charged Ni+2 affinity column pre-equilibrated with lysis buffer. After loading of supernatant, the Ni+2 column was washed with 10 column volume (CV) of lysis buffer followed by 10 CV of imidazole buffer (50 mM Tris-HCl, 250.0 mM NH_4Cl, 50.0 mM imidazole and 10 % glycerol; pH 7.5), followed by 10CV Urea buffer (50 mM Tris-HCl, 250.0 mM NH_4Cl, 1.0 M Urea, 10.0 mM imidazole and 10 % glycerol; pH 7.5) 10 CV of high salt buffer (50 mM Tris-HCl, 1.0 M NH_4Cl, 10.0 mM imidazole and 10 % glycerol; pH 7.5), before eluting the protein off the column using 10 CV of before elution buffer (50 mM Tris-HCl, 250.0 mM NH_4Cl, 50.0 mM EDTA and 10 % glycerol; pH 7.5). Elution fraction collected was then used for analyzing the presence of protein using denaturing SDS-PAGE gel (4 % stalking, 15 % separation gel), visualized by Coomassie staining. Eluted fractions (~ 10.0 mL) were then filled in to a dialysis cassette (10,000 MW) and dialyzed twice, using 1 L of dialysis buffer (50 mM Tris-HCl, 250.0 mM NH_4Cl and 10 % glycerol; pH 7.5) at 4 °C or in cold room, with gentle spinning. Dialyzed protein was kept on ice and filtered using 0.2 micron syringe filter before determining the concentration of protein using $A_{280/260}$ ratio. Protein is then diluted, if needed, 1.0 – 1.5 mg/ml concentration and stored at – 20.0 °C for future usages. Hfq is highly stable at – 20.0 °C and can be stored for years for future usages.

Expression and purification of His-6 tagged T7 RNA polymerase: BL21(DE3) carrying the expression plasmid for His-6 tagged T7 RNA polymerase was a kind gift from Dr. Christine Chow lab. Expression cells (from Dr. Chow lab stock) were streaked on a LB-Agar-Ampicillin (100 µg/ml) plate. 5.0 ml LB-media was inoculated with cells picked from the single colony. The

overnight culture was then used to inoculate fresh 1 L of LB-media containing Ampicillin (100 µg/ml) and cells were grown (250 rpm @ 37 °C), until OD_{600} of 0.4–0.5 have been reached. Cells were induced with IPTG (final concentration of 1mM) to express the protein for 4–5 hours. Cells were harvested (5000 g, 10min @ 4 °C) and cells pellet was stored in @ –20 °C until ready for purification.

Cell pellet was thawed on ice and then suspended into ice cold lysis buffer (50 mM Tris-HCl, 500.0 mM NaCl, and 20.0 mM imidazole; pH 8.0) up to the volume of 15.0 – 20.0 ml. Half a tablet of proteases inhibitor cocktail (ROCHE, complete from Sigma – 11697498001) was added and the lysis was done by sonication (4–5 cycles of 30s pulse with 1.0 min pause @ 37 % amplitude). Lysed cells suspension was then clarified to obtain the clear supernatant by centrifugation (30,000 rpm for 45 min @ 4 °C, using JA-17 rotor). Clear supernatant was then filtered through 0.8 micron syringe filter and transported to cold room (2 – 6 °C) for further purification. The clear supernatant was loaded on to a charged Ni+2 affinity column pre-equilibrated with lysis buffer. After loading of supernatant, the Ni+2 column was washed with 10 column volume (CV) of lysis buffer followed by 10 CV of high salt buffer (50 mM Tris-HCl, 1.0 M NaCl, and 20.0 mM imidazole; pH 8.0), before eluting the protein off the column using 10 CV of before elution buffer (50 mM Tris-HCl, 500.0 mM NaCl, and 400.0 mM imidazole; pH 8.0). Elution fraction collected was then used for analyzing the presence of protein using denaturing SDS-PAGE gel (4 % stalking, 15 % separation gel), visualized by Coomassie staining. Eluted fractions (~ 10.0 mL) were then filled in to a dialysis cassette (10,000 MW) and dialyzed twice, using 1 L of dialysis buffer ((50 mM Tris-HCl, 500.0 mM NaCl in 50 % glycerol; pH 7.5) at 4 °C or in cold room, with gentle spinning. Dialyzed protein was kept on ice and filtered using 0.2 micron syringe filter before determining the concentration of protein using $A_{280/260}$ ratio. Protein

is then diluted, if needed, 1.0 – 1.5 mg/ml concentration and stored at – 20.0 °C for future usages. T7 RNAP is a stable protein and can be stored at – 20.0 °C for years for future usages.

Cloning of RNA constructs: To transcribe the selected RNA sequences via *in vitro* transcription, first the corresponding DNA sequences were amplified using the primers from table 2.3, following the temperature profile mentioned. The amplified PCR products were then analyzed using agarose gel and purified using PCR clean up kit, as mentioned in previous section. The PCR products and the pUC19 cloning vectors were then digested and ligated after clean up using T4-DNA ligase. The ligation mixture was then transformed into XL-10 or Top-10 *E. coli* strains. Single colonies were obtained after plating the cells post-transformation and grown @ 37 °C for 16 h. Single colonies were then picked for colony PCR to identify the presence of correct plasmid construct, using standard pUC19 sequencing primers. Plasmids isolated from selected colonies by miniprep were used to do sequencing PCR (Sanger sequencing) following Feig's lab standard protocol for DNA sequencing, using standard pUC19 sequencing primers. The sequencing PCR products were then cleaned and sequence analyzed using the SEQ 8000 sequence analyzer. Identified colonies carrying the constructs of interest were then stored in 50 % glycerol @ –80 °C for future usages. For list of constructed plasmids please check appendix I.

	Primes Name	Primers sequence (5'- 3')	DNA-polymer-ase used	Annealin-g temp (°C)	Elongati-on time (min)	Cycles	Restrcict-ion sites used for cloning	Restrcict-ion sites used for linearizat ion
1	hns-for	5' - ATT GAT GAA TTC TAA TAC GAC TCA CTA TAG GAA CAA ACC ACC CCA ATA TAA GTT TGA G -3'	Taq	60.8	1	30	EcoRI	--
2	hns-rev	5' - CTC AAT CTG CAG CTT AAG TTC TCT TGC CTG CGC AC -3'	Taq	58.4	1	30	PstI	AflII
3	glmS-for	5' - ATT GAT GAA TTC TAA TAC GAC TCA CTA TAG CGT CAC ATG GGA TGA GGA GAT AAC - 3'	Taq	58.9	1	30	EcoRI	--
4	glmS-rev	5' - CTC AAT CTG CAG CTT AAG ACC TTC AAG AAG GAT TTC TGC -3'	Taq	56.7	1	30	PstI	AflII
5	glmY-for	5' - ATT GAT GAA TTC TAA TAC GAC TCA CTA TAG GAG TGG CTC ATT CAC CGA C -3'	Taq	57.5	1	30	EcoRI	--
6	glmY-rev	5' - CTC AAT CTG CAG CTT AAG AAC AAA GCC GGG AAT TAC C -3'	Taq	56.3	1	30	PstI	AflII
7	glmZ-for	5' - ATT GAT GAA TTC TAA TAC GAC TCA CTA TAG CGT AGA TGC TCA TTC CAT CTC TTA TGT TC -3'	Taq	60.4	1	30	EcoRI	--
8	glmZ-rev	5' - CTC AAT CTG CAG CTT AAG AAA AAA AC CCT GCT CTT ATT ACG - 3'	Taq	59.4	1	30	PstI	AflII
9	ompC-for	5' - ATT GAT GAA TTC TAA TAC GAC TCA CTA TAG GTT GCC GAC TGA TTA ATG AGG G - 3'	Taq	58.6	1	30	EcoRI	--
10	ompC-rev	5' - CTC AAT CTG CAG CTT AAG GTT TGC TGC GCC TGC -3'	Taq	57.1	1	30	PstI	AflII
11	ompF-for	5' - ATT GAT GAA TTC TAA TAC GAC TCA CTA TAG GAG ACA CAT AAA GAC ACC AAA CTC T - 3'	Taq	59.5	1	30	EcoRI	--
12	ompF-rev	5' - CTC AAT CTG CAG CTT AAG TGC AGT ACC TGC TAC TAA CAG AG -3'	Taq	60.1	1	30	PstI	AflII
13	ryhB-for	5' - ATT GAT GAA TTC TAA TAC GAC TCA CTA TAG CGC GAT CAG GAA GAC CCT CG - 3'	Taq	60.4	1	30	EcoRI	--

	Primers Name	Primers sequence (5'- 3')	DNA-polymer-ase used	Annealin-g temp (°C)	Elongati-on time (min)	Cycles	Restrcict-ion sites used for cloning	Restrcict-ion sites used for linearization
14	ryhB-rev	5' - CTC AAT CTG CAG CTT AAG AAA AGC CAG CAC CCG G - 3'	Taq	57.7	1	30	PstI	AflII
15	rybB-for	5' - ATT GAT GAA TTC TAA TAC GAC TCA CTA TAG GAC TGC TTT TCT TTG ATG TCC CC - 3'	Taq	59.6	1	30	EcoRI	--
16	rybB-rev	5' - CTC AAT CTG CAG CTT AAG AAC AAA AAA CCC ATC AAC CTT GAA - 3'	Taq	59.9	1	30	PstI	AflII
17	sdhC-for	5' - ATT GAT GAA TTC TAA TAC GAC TCA CTA TAG CGT CTC CGG AAC ACC CTG C -3'	Taq	60.5	1	30	EcoRI	--
18	sdhC-rev	5' - CTC AAT CTG CAG CTT AAG GAA CCG GAT GGT CTG TAG G - 3'	Taq	57.4	1	30	PstI	AflII
19	rhlB-for	5'- TAT AGT CCA TGG GCA AAA CAC ATT TAA CAG AAC AGA AGT TTT CC - 3'	Taq	65.2	2.3	30	NcoI	
20	rhlB-rev	5'- TAT AGT AAG CTT ACC TGA ACG ACG ACG ATT ACG C- 3'	Taq	65.1	2.3	30	HindIII	
21	rhlB-int-for	5' - TAA TAC GAC TCA CTA TAG G - 3'	Seq-kit*	50.9	4	25		
22	rhlB-int-rev	5' - CTA GTT ATT GCT CAG CGG - 3'	Seq-kit*	54.7	4	25		

Table 2.3 : List of primers used for cloning RNA constructs and the RhlB enzyme into pUC19 and pET28a vectors, respectively. The DNA sequences were picked from Top-10 E. coli strain. * Commercially available sequencing kit were used which comes with a ready to use reaction mixture containing DNA-polymerase.

In vitro transcription, purification and analysis of RNAs: All the template plasmids were linearized with the restriction enzymes mentioned in Table 2.3, and phenol:chloroform:iso-amyl alcohol (25:24:1; pH – 8.1) extraction was done twice followed by chloroform extraction and ethanol precipitation following the standard phenol:chloroform extraction procedure for DNA. The linearized templates were resuspended using autoclaved MilliQ water and the concentrations were measured using $A_{260/280}$ ratio to ensure the quantity and purity. *In vitro* transcriptions to prepare the required RNAs were done using Dr. Feig's lab transcription protocol. T7 RNAP was purified as described in previous section and test reactions (40.0 mM Tris-HCl, 15.0 mM $MgCl_2$,

0.01% Triton X-100, 2.0mM spermidine, 5.0mM DTT, 2.0 mM of each NTP (ATP, CTP, UTP and GTP), 20 ng of linearized plasmid templates and 1 µL of T7 RNAP (1.3 mg/ml)) were set up at 37 °C for 1 h. Upscale *in vitro* transcription reactions (20.0 mL reaction volume) were set-up following the same protocol as test transcriptions except that for 20.0 mL reactions only 100–200 ng of linearized template DNA and 50 µL of T7 RNAP were used for each reaction. Reactions were incubated for 4 h @ 37 °C with intermittent shaking and spin (1000 rpm). RNAs were precipitated (using 0.5 M NH_4OAc (pH 5.2), 100 % ethanol (3X to reaction volume) @ –20 °C). RNA obtained were further purified using denaturing Urea-PAGE gel (7.0 M Urea, 8% PAGE gel) following standard purification protocol. The RNAs obtained were resuspended and quantified using $A_{260/280}$.

Coupled enzyme assay for ATPase activity detection: To determine the ATPase activity of RhlB and RhlE, lactate dehydrogenase/pyruvate kinase coupled enzyme assays were done. Depletion of NADH was monitored at the wavelength 340 nm. The concentrations of reagents used in the assays were as mentioned in table 2.4.

Measurement were made using UV-Vis 8453 spectrophotometer (Agilent), over a reaction time of 10.0 min and repeated measurement were taken at every 30s. Effects of Hfq was study at by adding Hfq (100 nM) to each reaction containing 200 nM of substrate RNA. 25.0 nM and 50.0 nM of RhlE and RhlB has been used in both Hfq +/– reactions. A reaction without RhlB or RhlE was considered as background. Spectroscopic data were analyzed using Kaleidagraph and Microsoft Excel.

Reagents	Stock Concentration	Final Concentration
HEPES (pH 7.5)	500 mM	10 mM
KCl	500 mM	75 mM
$MgCl_2$	20 mM	2.0 mM
ATP	100 mM	1.25mM
Phosphoenol Pyruvate	5 mM	0.2 mM
NADH	10 mM	0.15 mM
PK	500 u/ml	10 u/ml
LDH	1000 u/ml	20 u/ml
Substrate RNAs	500 nM	200 nM
RhlB or RhlE		25–50 nM
Hfq (in + Hfq rxns only)		100 nM

Table 2.4: List of coupled enzyme assay's components and concentrations.

Chapter 3: TcdA protein chimeras as cell-specific protein cargo delivery system

3.1 Introduction:

The targeted cellular delivery of drugs and proteins has tremendous scientific and therapeutic potential. *In vitro* delivery could lead to the better understanding of different signaling pathways, manipulation, and optimization of certain pathways for new therapeutic approaches, and/or generation of stem cells from pluripotent cells to name few. Similarly, *in vivo* delivery of a protein could replace or complement a lowly expressed, dysfunctional or unexpressed protein and hence giving a better control over cellular machinery or to help overcome deficiency related anomaly. However successful delivery of functional proteins across the cellular membrane is a very challenging task; for example: cell membrane largely keeps proteins from entering the cells, whereas endosomal isolation and degradation of proteins entering through vesicle formation could make it unproductive.[135-137] Several approaches have been developed to address these challenges such as (a) knocking out the target gene(s), and (b) conditional expression of protein via plasmid DNA transfection and expression of the protein using inherent cellular machinery. Using these methods, however, has their own drawbacks such as knocking out a gene could potentially to knock out or incorporate an undesirable sequence. Also, controlled expression of a protein to the biologically relevant level using in-situ Tetracycline or T7/lac responsive elements is difficult and requires optimization at multiple steps.[138-139] Another popular approach is a carrier-based approach, where biologically active molecules are directly delivered to the target cells using a carrier molecule. Usages of (a) cationic cell-penetrating peptides (CPPs), (b) supercharged proteins, (c) virus-like particle, (d) nano-particles, (e) liposomes and (f) polymers, are common

among several other carrier based protein delivery methods (**Fig 3.1**).[135,140] All these methods have their own limitations and a lot has to be done before these could be used as reliable carriers. For

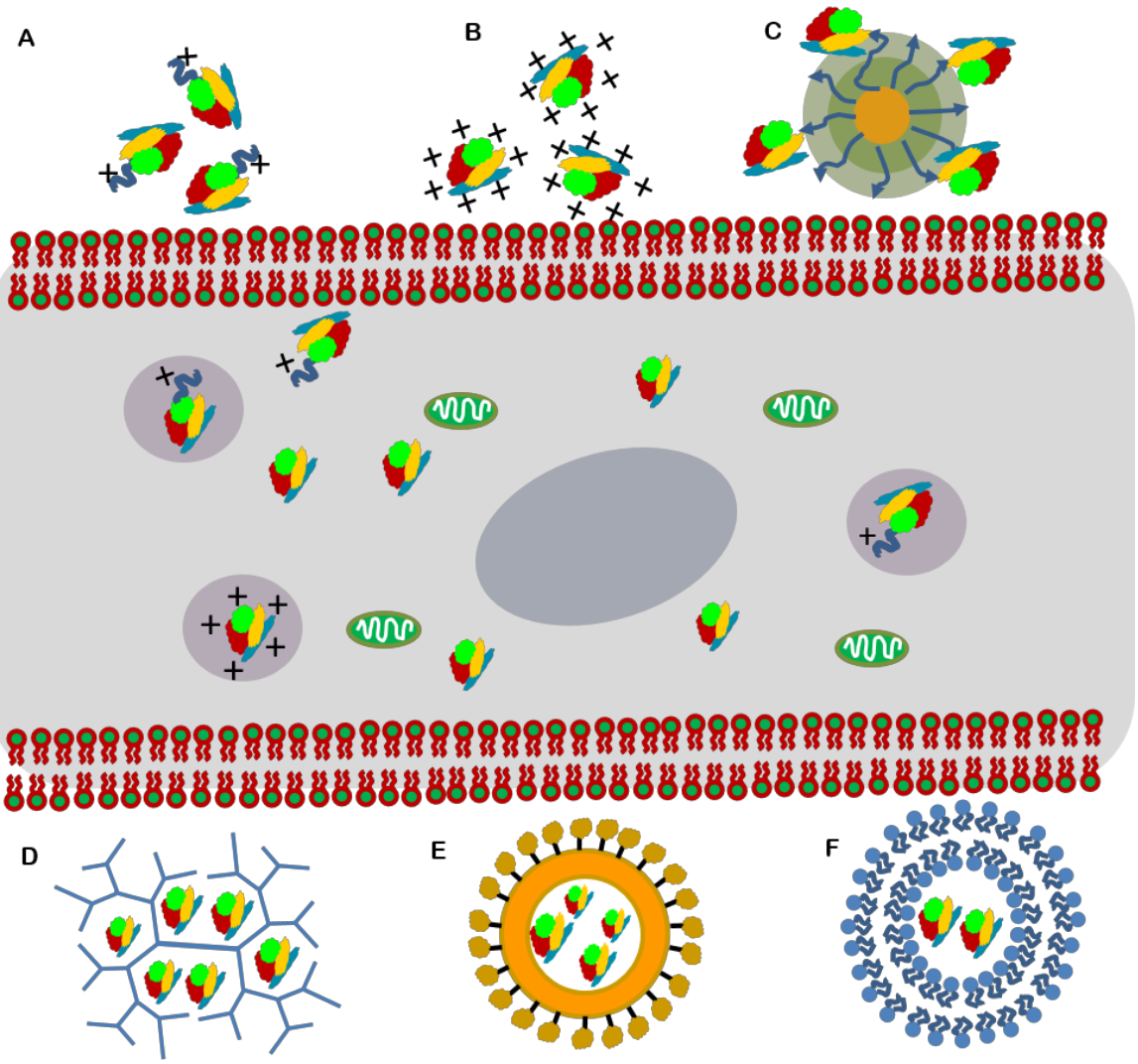

Fig. 3.1: Schematic illustration of popular protein delivery systems. (A) Cell penetrating peptides appended to the cargo protein, (B) supercharged protein, (C) nanoparticle carriers of proteins, (D) polymeric carriers, (E) virus-like particles loaded with cargo protein, and (F) Liposomal delivery of protein. Between two lipid bilayers nucleus (light blue eclipses), mitochondria (green eclipses) and the endosome (purple circle with entrapped protein) represent the cellular matrix and the general idea of cellular delivery of proteins.[135]

example: CPPs have been used frequently for cellular delivery of proteins. CPPs are efficient in the cellular delivery of proteins when appended to the cargo protein but using CPP as a delivery

system has its own shortcomings. Nuclear delivery of CPP appended cytosolic proteins are one of the most undesirable outcomes. CPPs have shown higher cell toxicity and off-target effects. Besides attaining the cellular specificity in a real-life sample, cytosolic availability of the cargo proteins in their target cells is another challenge.[136-137] Most carriers mediated cargos get trapped in the endosome and hence get degraded or unavailable to the cytosol to perform the desired functions. Therefore, there is a need for a cellular delivery system which can deliver big and/or small molecules and proteins across the cell membrane efficiently, and could also ensure the substantial cytosolic delivery of the cargo protein.

Bacterial exotoxins have evolved with high target specificity and effective delivery of functional domains in sufficient quantities to modulate the cellular functions. Exotoxins from different bacteria adopt different mechanisms for targeted delivery and to escape the vesicle entrapment.[141-142] Several studies have modified exotoxins to attain enhanced cellular targeting specificity and delivery of small proteins **(Table 3.1)**.[143-150] To achieve higher cellular specificity and delivery of protein/small-molecule using an exotoxin based carrier our lab focuses on developing a cargo delivery system which should be

a) Specific: for targeting specific cells
b) Non-toxic: the carrier should not affect the host cellular machinery
c) Efficient: substantially cytosolic delivery of cargos and availability to bring the desired effect.
d) Versatile: ideally the vehicle should be able to take any cargo irrespective of the size and origin and should be able to deliver it across the membrane.
e) Traceless: post-delivery, the transporter should be easily degradable by the cell so that it should not cause any non-targeted cellular activity

f) Easy to use: the simplicity of design and ease in preparation and handling would allow the widespread use of the technology from research to the treatment of diseases.

Toxins	**Cargo delivered**	**Ref.**
Clostridium botulinum toxin (*C. botulinum*)	Targeted secretion inhibitor delivered to pituitary somatotroph cells	149
Diphtheria toxin (*C. diphtheriae*)	Diphtheria toxin catalytic domain delivered to interleukin-2 receptor expressing malignant T-lymphocytes	116
Exotoxin A (*P. aeruginosa)*	*P. aeruginosa* exotoxin A catalytic domain to treat hairy cell leukemia	145
Clostridium difficile toxin-B (*C. difficile*)	Alkylguanine DNA transferase (AGT) to neuronal cells	143
Clostridium difficile toxin-A (*C. difficile*)	Gaussia luciferase to vero cells	150
Anthrax toxin (*B. anthracis)*	Diphtheria toxin catalytic domain delivered to EGF receptor expressing A431 cells	148

Table 3.1. Exotoxins engineered to prepare cargo delivery systems.

Our cargo delivery system design takes inspiration from the virulence factors or toxins of nasty nosocomial pathogen *Clostridium difficile*, also known as *Clostridium difficile* toxin A and B (TcdA/B) respectively. For the cargo delivery system design, our lab chose TcdA as explained below.

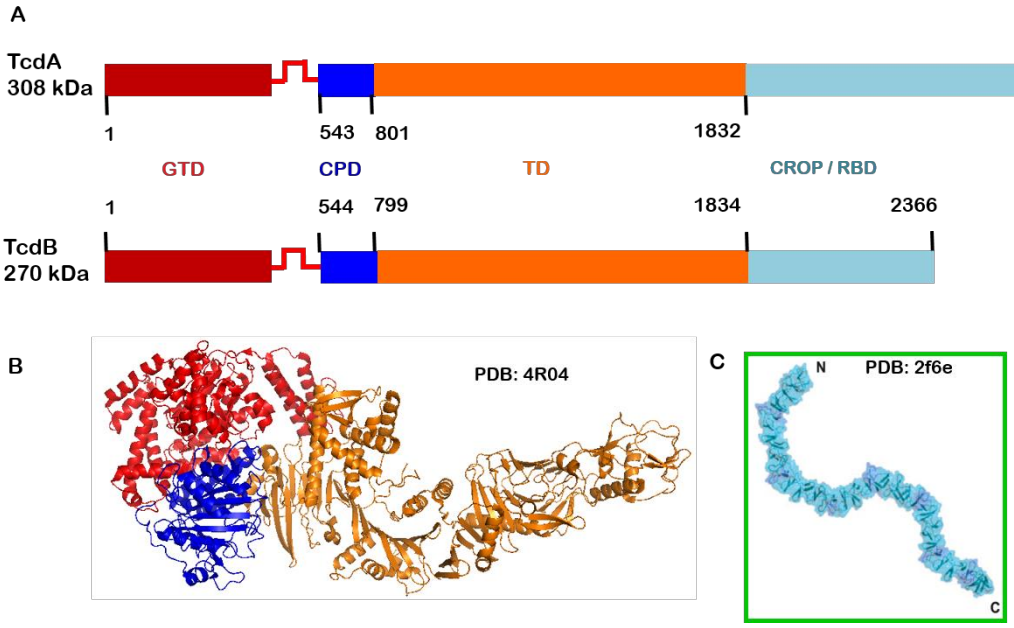

Fig 3.2: ***Clostridium difficile*** **enterotoxins A/B.** (A) Domains of enterotoxin A (TcdA) and enterotoxin B (TcdB) are shown from N- terminal to C-terminal; glucosyltransferase domain (GTD; maroon), cysteine protease domain (CPD; blue), translocation domain (TD; orange) and C-terminal repetitive oligopeptide (CROP; cyan). (B) Crystal structure of TcdA without CROP;[19] domains are color coded as in (A), (C) CROP structure predicted from NMR-spectroscopy data.[20,21]

3.2 Tuning TcdA into a noble protein delivery system:

Clostridium difficile (*C. difficile*) is a nosocomial, opportunistic pathogen which affects patients largely under prolonged antibiotics treatment. *C. difficile* infects and thrives on the compromised immunity and depleted gut micro-flora of a patient.[151-152] Upon infection, *C. difficile* secrets two major virulence factors known as Enterotoxin A and Enterotoxin B (TcdA and TcdB). Both TcdA and TcdB contain three distinct regions; (a) head: Glucosyl transferase domain (GT-domain; enzymatic part), (b) body: consists of cysteine protease domain (CPD) and translocation domain (TD) and, (c) tail: known as CROP **(Fig 3.2).**[151–155] Both TcdA and TcdB have a high structural and sequence similarity except that CROP region of TcdB is considerably smaller than TcdA. For further discussion, TcdA will be used owing to its relevance to the current study and,

the similar mechanism of infection and striking structural homology among TcdA and TcdB. The CROP region binding and aggregation to the surface receptors leads to the signaling and internalization of TcdA via endocytosis. Upon acidification, highly acidic pH of endosome leads to a conformational change in the translocation domain allowing it for threading through the endosomal membrane into the cytosol exposing the GT and CPD. CPD then releases the enzymatically active GT-domain to the cytosol via an autolytic cleavage in the presence of inositol hexakisphosphate, in the cytosol. Further, GT-domain catalyzes the glucosylation of the Rho family GTPases resulting in cell death. Endosome encapsulated part of the toxin gets digested and

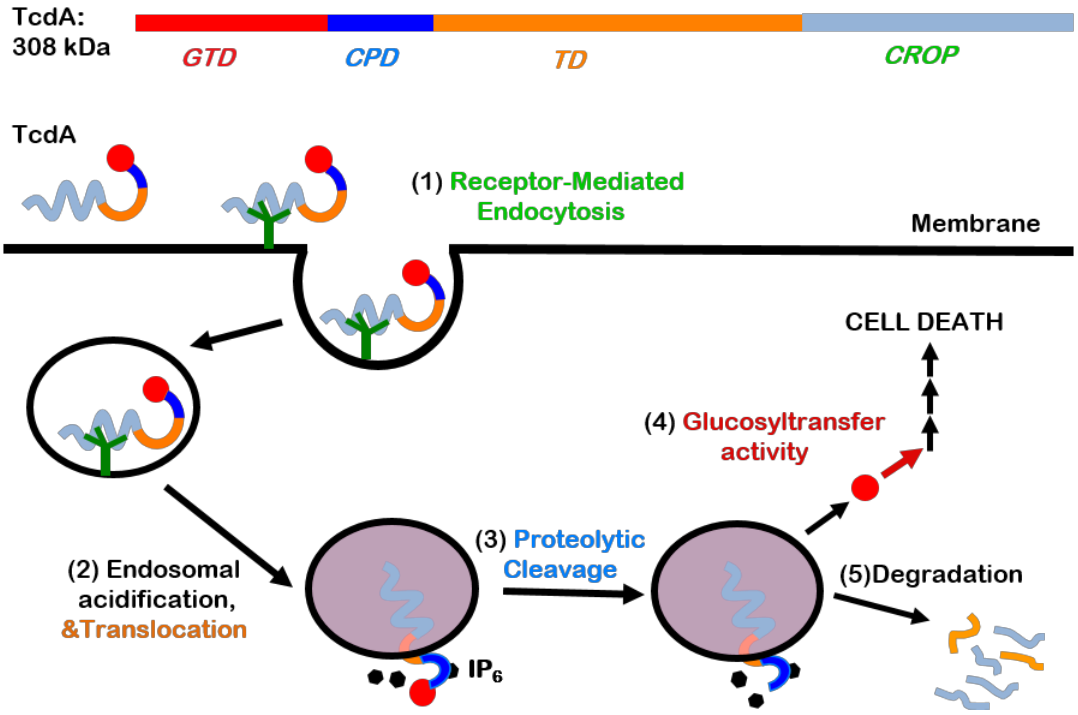

Fig 3.3: Schematic illustration of etiology of *C. difficile* toxins A/B(TcdA/B). TcdA has been used in scheme to the context of the details in text. (1) Crop binding to the cell surface receptor leads to the aggregation and internalization of TcdA via endocytosis, (2) Endosomal acidification leads to the conformational change of TD leads to threading out of GT and CPD, (3) self-cleavage of CPD in presence of IP_6 (black hexagons) releases the GT into cytosol, (4) GT mediated glucosyltransferase activity ultimately leads to cell death, meanwhile (5) the remaining part of TcdA in endosome degrades over time.[151]

hence leaves no traces **(Fig 3.3).**

Inspired by the natural ability of TcdA to efficiently transduce the GT-domain, our lab prepared "cargo-TcdA/B" chimeric constructs as protein carriers. As a proof of concept, Emerald GFP and *Gaussia luciferase* genes were used to replace GT-domain of TcdA. The chimeric proteins were expressed using *Bacillus megaterium* (*B. megaterium*) expression system and the efficiency of toxin chimeras to deliver the cargos (Emerald GFP and *Gaussia* luciferase proteins) were measured. Luciferase chimera (Luc-TcdA) was delivered into cytosol with an efficiency of 50% whereas Emerald-GFP was unable to be released into the cytosol. The punctuate staining of cells incubated with Emerald-GFP lead to the speculation that the stable structure of Emerald-GFP does not allow it for threading out of the endosome. While for Luc-TcdA no internalization of chimera was observed at 4 °C but with the temperature being shifted to 37 °C the internalization

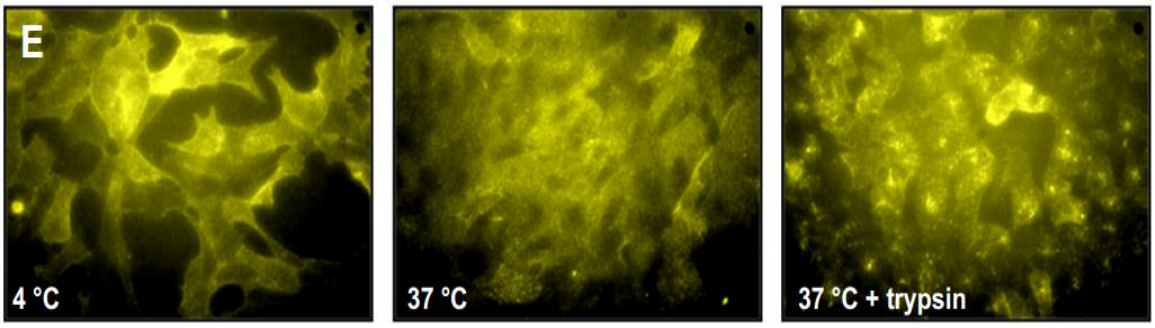

Fig 3.4: Internalization of Luc-TcdA chimera studied by immunostaining using vero cells. (A) Incubation of vero cells with Luc-TcdA at 4 °C leads to the binding of chimera on cell surface without internalization as internalization is frozen/seized at lower temperature. (B) The temperature raise from 4 C to 37 C facilitated the internalization. (C) Cells were treated with trypsin at 37 C to remove cell surface bound chimera, therefore the immunostaining shows only internalized chimera. Punctate staining was suggested to be the endosome entrapped chimera.[150]

of Luc-TcdA occurred. Further cytosolic delivery of Luc-TcdA was confirmed by cyto-immunostaining **(Fig 3.4)**.[150] Estimated 50% efficiency was achieved as far as delivery of Luc-TcdA is concerned as mentioned above. Similar to our lab's Luc-TcdA chimera, Krautz-Peterson G et al. have used TcdB as a cargo delivery carrier where cell specificity was attained using botulinum neurotoxin receptor binding domain (RBD) to a neuronal cell. Also, they appended the

cargo, an alkyltransferase, N-terminal to the GT-domain of TcdB, to prepare the AGT-TcdB-BoNT/A-Hc.[143]

3.3 Chimeric Cargo-Toxin-Receptor binding domain: innovation, design, and approach

Our current work focuses on developing the existing Luc-TcdA in an easily adaptable delivery system. The aim was to develop a carrier construct on which cargos, as well as RBDs, could be swapped easily for versatile use and efficient expression. Significant design elements have been introduced to ensure the accomplishment of these properties. First, we added BamHI and SpeI restriction sites to the N-terminal and C-terminal side of the body (CPD + TD) of TcdA. Insertion of these two restriction sites gives us the ability to switch the cargo and/or RBD with our choice of cargo and RBD in any existing chimera construct. Second, a Ybbr12-tag (13 amino acids sequence) was introduced at the C-terminus of cargo peptide and prior to the CPD cleavage site was also introduced. This tag will allows us to add a fluorophore/biotin label to the cargo using the Sfp enzyme which in turn would help us track/pull-down the released cargo domain in the cytosol for qualitative and quantitative estimation.[156] Third, our innovation was to add a sortase-tag to the C-terminus of CROP/RBD regions prior to an existing His-6 tag, which is used for purification of protein using affinity chromatography. The Sortase tag will allow us to add a second fluorophore label to the protein using the SrtA enzyme.[157] Additionally, upon transfer of the fluorophore label to target sortase tag the His-6 tag will be released allowing us to easily separate the labeled protein (His-6 tag absent) from unlabeled protein (with his-6 tag) using one step Ni affinity chromatography. Together the YbbR-12 and Sfp tags give us the ability of orthogonal labeling of the chimera along with better purification and in situ tracking.

Multiple cargos were selected for this study. Bcl-2-associated X protein and Caspase 9 are pro-apoptotic and apoptosis inducer proteins, whereas an X-linked inhibitor of apoptosis (XIAP)

and Cyclin-dependent kinase 5 activator (p35) are apoptosis inhibitory proteins. Apoptosis or inhibition of apoptotic behavior by the cargos would provide a convenient visual mean for qualitative and quantitative estimations of the delivery of active cargos. Vascular endothelial growth factor (VEGF), epidermal growth factor (EGF) and the heavy chain of Botulinum neurotoxin A(BoNT/A) were our choices for the RBDs. Commercial availability of multiple cell lines exhibiting the positive and negative phenotypes of the RBDs' specific receptor makes easy to explore and compare the cellular specificity of different chimeric constructs.

Our chimera design **(Fig: 3.5)** allows swift swapping of the cargo and/or RBDs hence allows preparation of a chimera library where multiple cargos chimera can be constructed keeping the RBD unchanged, or vice-versa. All together the finished set of our chimeric proteins, (a) would allow us to prove the versatility and easy maneuverability of our constructs, (b) would allow us to compare the efficiency and effects of different RBDs on delivery of a cargo, and vice-versa, hence several layers of information could be obtained conveniently.

Cloning of huge a chimera plasmid (>14 kbp after final cloning) was challenging and took meticulous planning. To make the cloning process easy several sub-cloning steps were required. Cargos and RBDs were first cloned separately and then assembled together at final step **(Fig 3.6).** The same cloning scheme was followed to assemble all the chimera and hence to avoid the repetition, cloning of Bax*-TcdA-CROP will be explained here as a representative clone. Bax* was made by site-directed mutagenesis of a single nucleotide to remove the BamHI restriction site inherited in Bax sequence, without changing the amino acid residue. Final verification for all the chimera assembly was done by sequencing and the list of chimeric construct prepared can be found in appendix II. First, the Bax* gene was amplified, from the corresponding parent vectors, using the cargo specific primers to introduce specific restriction sites and the Ybbr-12 tag. The amplified

Bax* was cloned into the pCR2.1®TOPO® TA vector (TOPO). Colonies of interests were identified by the colony-PCR (cPCR) using TOPO specific sequencing primers. Colonies carrying

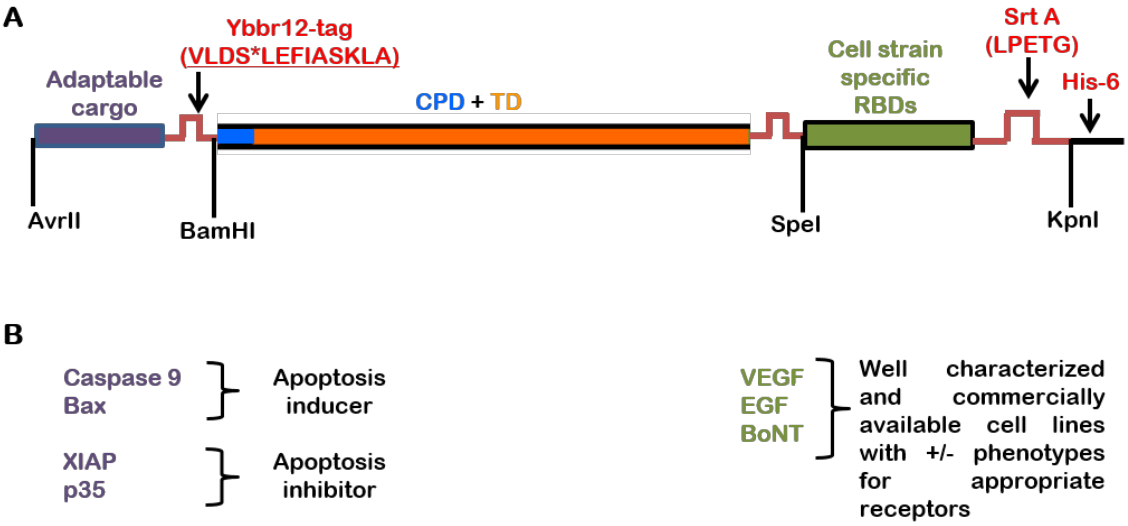

Fig 3.5: Chimera design with adaptable/replaceable cargo and RBDs. (A) Replaceable cargos (purple) and RBDs (green) were engineered into the chimera constructs by introducing unique restriction sites shown. Cargos were cloned with YbbR-12 (a 13 amino acids peptide tag) and RBDs were cloned with a sortase tag to provide handles for orthogonal labeling and purification. (B) List of cargo and RBDs used to prepare the chimera (cargo-TcdA-RBD) constructs.

right plasmid construct and sequence of the insert were identified by sequencing the plasmid DNA. The Bax-TOPO construct and plasmid pWH1520* were digested using AvrII and BamHI and were then ligated together. Identification of colonies carrying the plasmids with right inserts was done by cPCR using the pWH1520* specific primers. pWH1520* is our lab modified (prepared by Dr. S. Kern) version of a commercially available pWH1520 plasmid which has been used successfully to clone and express Luc-TcdA and EGFP-TcdA chimeras.

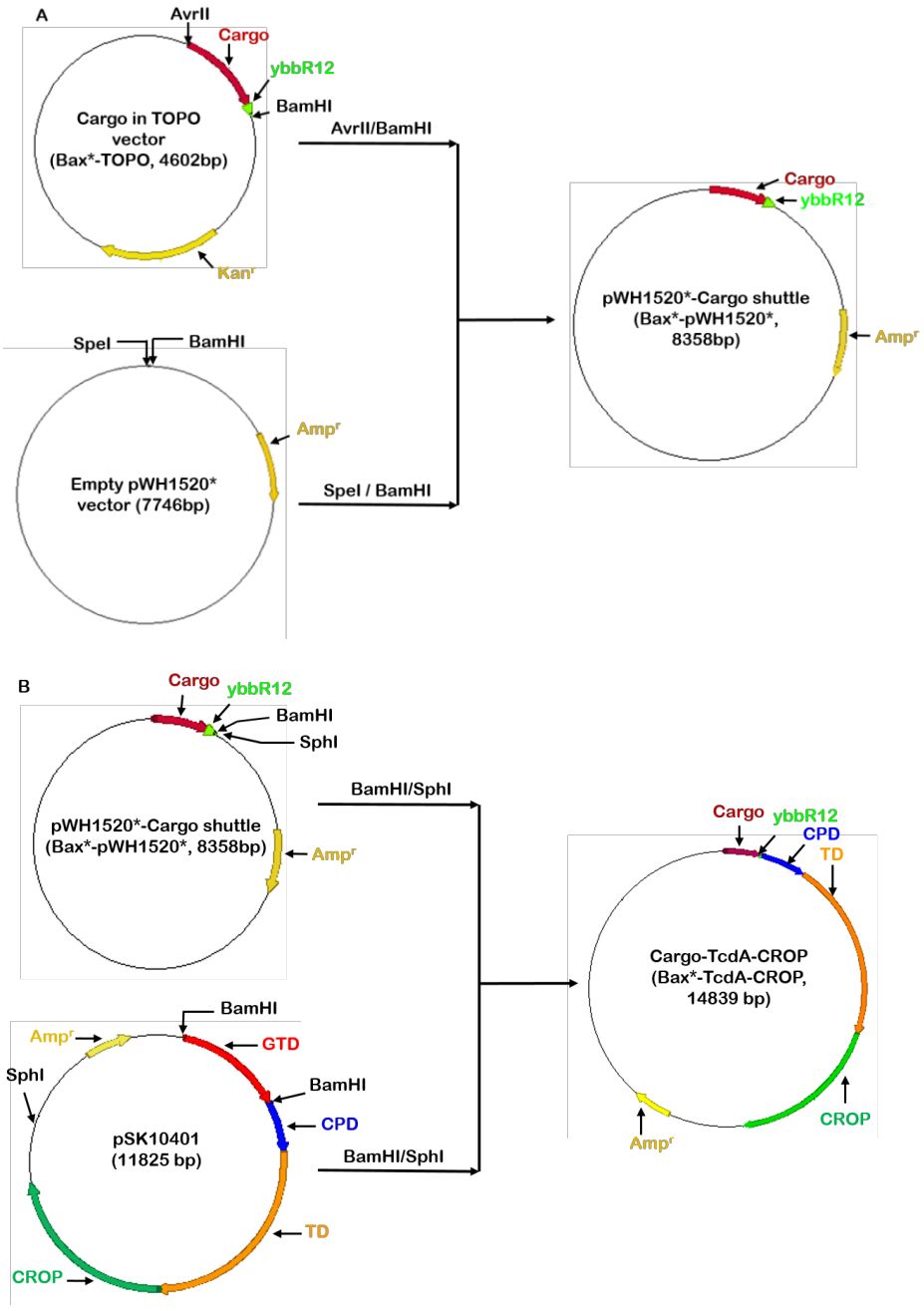

Fig 3.6: Cloning strategy to prepare the Cargo-TcdA-CROP (A) Cargos Bax*, Casp 9, XIAP and p35 were cloned from corresponding parent vectors and cloned into TOPO. Resulting cargo-TOPO vectors were digested with AvrII/BamHI and the inserted into pWH1520*. (B) pWH1520*-Cargo shuttle and plasmid pSK10401 were then digested with BamHI/SphI. Fragments were gel purified to obtain clean fragments of desired length which were then ligated to prepare Cargo-TcdA-CROP plasmids. Cargo-TcdA-CROP plasmids were used for both expression of Cargo-TcdA-CROP, as well as shuttle vector to be used for Cargo-TcdA-RBD plasmid assembly.

In the third step of cloning, the pWH1520*-Bax plasmid and pSK10401 (pWH1520* carrying *wt*TcdA) were digested with SphI and BamHI. Restriction digestion of both plasmids resulted into multiple fragments. Correct sized fragments were isolated using Agarose-gel separation and purification method. Isolated fragments were ligated together, transformed and single colonies obtained were used to miniprep the plasmid DNA carrying Bax*-TcdA construct. Correct colonies were identified by restriction digestion of plasmids obtained from miniprep **(Fig 3.7).** Parallel to cargos, the RBDs were being cloned by Adam Boyden following similar strategy which resulted into RBD-shuttle (RBD in pWH1520*). Final assembly of Bax*-TcdA-RBD was done by Adam Boyden. Briefly, the Bax*-TcdA and RBD-shuttle were double digested with SpeI and XhoI followed by isolation and ligation of the desired bands. Transformation of ligation

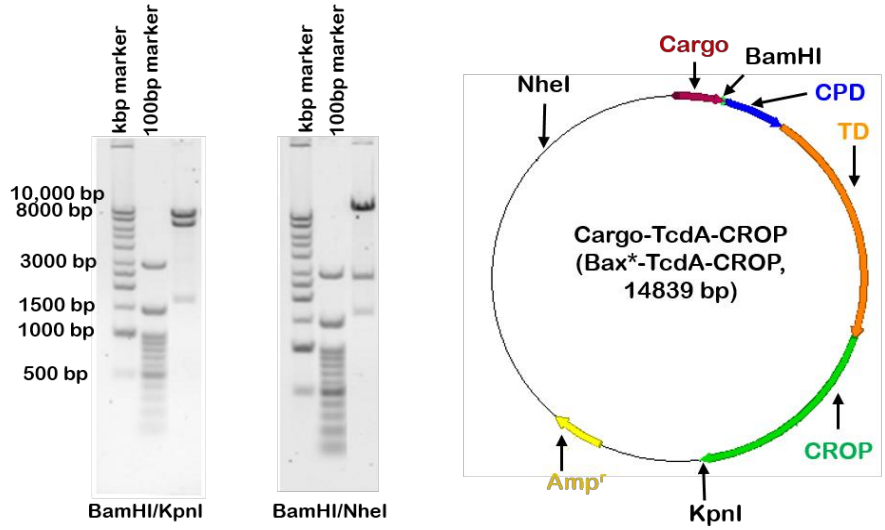

Fig 3.7: Restriction double digest analysis of cargo-TcdA construct (Bax*-TcdA-CROP) using BamHI/KpnI (left) and BamHI/NheI (middle), and the plasmid map indicating the relative position of the digestion site. 100 bp marker and kbp marker were used (there is no 7000 bp band in the marker)

product yielded single colonies from which colonies of interest were identified primarily by cPCR. Following the cPCR, plasmids were isolated and restriction digested to identify the possible

colonies for sequencing. Final confirmation was done by sequencing the plasmids. All the cloning including the sequencing of the final Bax*-TcdA-RBD construct, prior to expression, were done in Top-10 *E. coli* strain. Primers used for the cloning of cargos and the sequencing of plasmids at different stages of chimera construct preparations could be found in appendix III and appendix IV, respectively. *Bacillus megaterium* (*B. megaterium*) was the organism of choice to express the chimera proteins.

3.4 Expression of protein chimera and troubleshooting

As mentioned above *B. megaterium* has been used for the expression of all the chimeric constructs prepared. *B. megaterium* was chosen based on previous success in expressing large proteins (~300 kDa), Luc-TcdA and EGFP-TcdA chimeras. It also lacks endotoxins, which is a desirable trait for expressing the proteins required for testing on human cell lines. Finally, the Bax*-TcdA-CROP construct was transformed into *B. megaterium* and tested for the expression. The standard growth and purification conditions to grow and express the Bax*-TcdA-RBD as used for Luc-TcdA and EGFP-TcdA was followed as reported by Dr. Stephanie Kern. Briefly, protein purification was done using the standard Ni column affinity chromatography procedure followed by size exclusion chromatography (SEC). A second Ni column chromatography step was used to concentrate the diluted protein fractions obtained from SEC. First few attempts to purify the proteins do

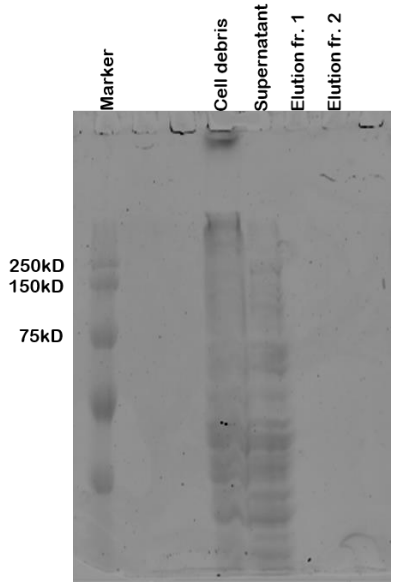

Fig 3.8: Cargo-TcdA-CROP chimeric protein purification was done following the protocol same as Luc-TcdA. 5 µL of protein ladder, cell debris and supernatant and 10 µL of elution fractions (after first Ni affinity column) were loaded in the corresponding lanes. SDS-PAGE gel was stained with Coomassie stain for visualization. No evidence of Bax-TcdA protein was found.

not yield any visual evidence of the presence of Bax*-TcdA-RBD analyzed on SDS-PAGE gel and stained with

Coomassie stain **Fig 3.8**. To rule out the error in purification procedure or technique, parallel to me Adam Boyden also tried to purify XIAP-TcdA-EGF (XAE) chimera which yielded no protein either. After attempting several growth and induction conditions for chimeric protein expressions, there was no evidence of expression of protein. Our protein chimera has eukaryotic protein domains as cargos and RBDs. Expression of these proteins could be affected by the low relative abundance of tRNAs in *B. megaterium*. A codon bias analysis (done by me and Adam Boyden) shows that there is a high negative codon bias for 5 or more codons towards all the cargos and RBDs chosen for the study, except for the cargo XIAP. It is interesting to notice that the *wt*-TcdA protein was being successfully expressed even though it contains 2, 5 and 8 codons with high negative bias in GT-domain, CPD and Translocation domain, and CROP respectively. Also, BoNT/A which has been used as RBD domain by Feng group has 5 codons which show high negative codon bias when compared to *B. megaterium* codon usage. Based on this information, **we hypothesized that the heavy negative codon bias to the N-terminal end of the protein could disrupt the protein translation and hence no protein is being observed in our purification attempts.** Since XIAP shows no codon bias and the previous success with the purification of *wt*-TcdA (with *wt*-CROP) makes XIAP-TcdA a strong candidate to test the expression of the chimeric protein. The XIAP-TcdA chimera was transformed in *B. megaterium*. XIAP-TcdA chimera was grown and expressed like Bax*-TcdA-RBD and the purification was done using Ni column chromatography. There was no protein visible when purification samples were analyzed on SDS-PAGE gel. To further verify, the expression of protein chimera, XAIP-TcdA was expressed and analyzed by western blot using rabbit anti-His-6 primary and a horseradish peroxidase substrate

conjugated anti-rabbit-goat secondary antibody. The control lane was loaded with purified wt-TcdA. As evident form **Figure 3.9**, no protein was found in lane loaded with XIAP-TcdA.

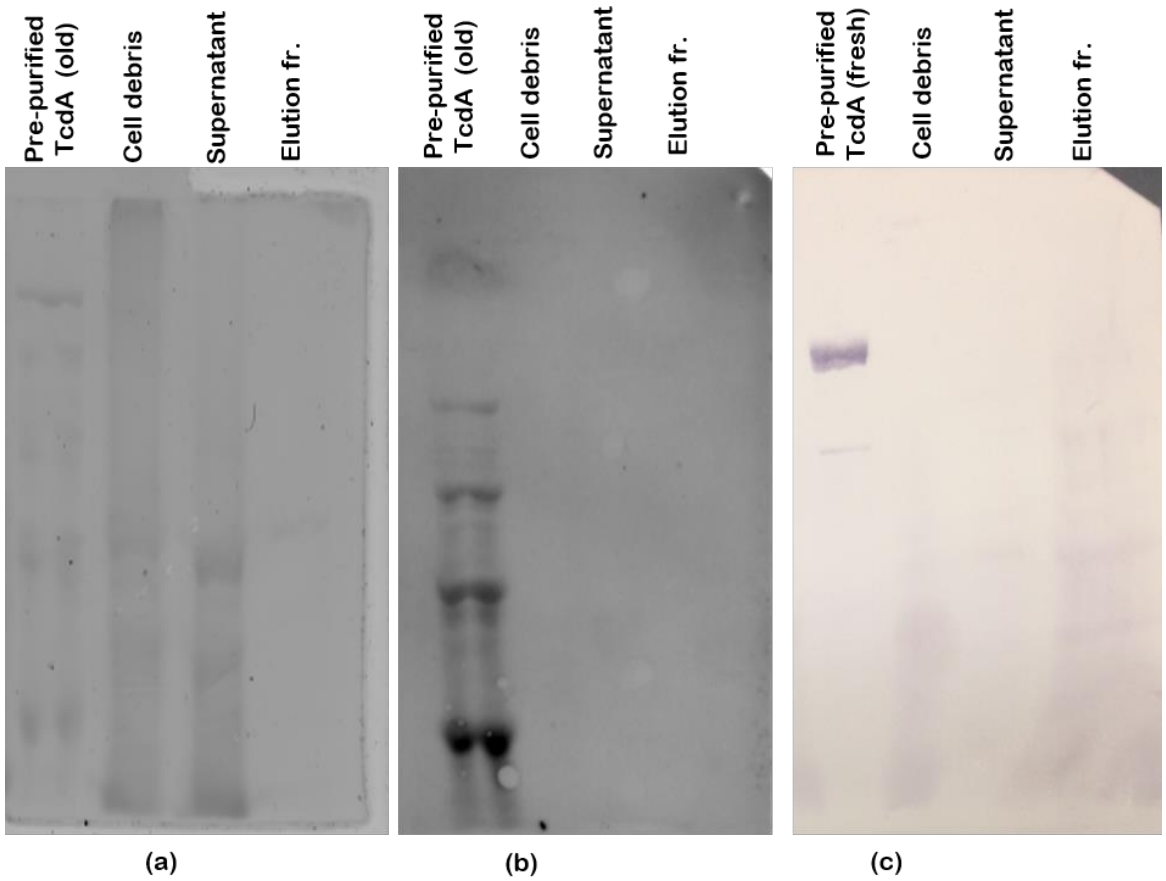

Fig 3.9: Western blot analysis of XIAP-TcdA-CROP chimeric protein expression. XIAP-TcdA-CROP purification was done following the protocol same as Luc-TcdA. 5 µL of cell debris and supernatant and 10 µL of elution fraction (after first Ni+2 coulmn) were loaded in the corresponding lanes. Pre-purified TcdA-His6 was used as control. (a) SDS-PAGE gel was stained with coomassie stain for visualization. (b) and (c) are wester blot image done using PVDF membrane, and the blot was developed using rabbit anti-His-6 monoclonal antibodies and goat anti-rabbit secondary antibodies conjugated with HRP. SDS PAGE gel for (a) and (b) were ran as duplicates. (c) only one gel was ran to do the western transfer shown in (c).

At this point, the failure of the system to express the protein from a perfect looking plasmid construct is up for debate. The plausible reasons could be the codon bias, which is highly debatable comparing the codon bias of *wt*-TcdA to XIAP-TcdA. Another likely speculation could be the

instability of the transcript of eukaryotic domains because of misfolding or lack of chaperone proteins contributing to the folding and stability of the transcripts. Nonetheless, the analysis and efforts made to fix the issue of chimeric protein expression have not yielded into a successful expression.

Chapter 3: Materials and methods

Cloning of Cargos in TOPO vector: Bax and p35 were PCR amplified out of the commercial vectors. XIAP and Caspase 9 parent vectors used for amplification of corresponding cargos were kind gifts from Dr. Dukett Lab at University of Michigan. Primers 1–8 were used and the corresponding temperature profile (melting, annealing and elongation temperature) for each amplicon as mentioned in table 3.2. Pfu polymerase (1X Pfu buffer: 0.8 mM dNTPs, 0.2 µM individual primers concentration, 1 µl of Pfu from 1.6 mg/ml stock) was used for all the PCR amplifications and 10–50 ng/50 µl of template DNA was used per PCR reaction. For cloning the amplicon from the first step of PCR reactions, amplicons were first purified using EZNA Microelute cycle-Pure Kit (Omega, D6293-03). 250 ng of purified PCR product was set up for a Taq-polymerase (Fisher Scientific, 1X Taq buffer, 2.5 mM $MgCl_2$, 0.8 mM dNTPs and 1 U Taq-polymerase/10 µl reaction) at 72 °C for 5 min extension. The Taq-polymerase reaction was then used for ligation with pCR2.1®TOPO®TA vector (Invitrogen) following the manufacturer's protocol. The ligation mixture was transformed into TOP-10 *E. coli* electrocompetent cells via electroporation using Bio-Rad micropulser and plated on LB-Agar plates with Kanamycin (30 mg/ml). Single colonies obtained were used to verify the right clone by cPCR using TOPO vector-specific forward and reverse primers (annealing temperature 48 °C, using Pfu-polymerase and same extension time as used for amplifying the targets from commercial vectors mentioned in table 3.2) and analyzed by gel electrophoresis using 1.0–1.5 % Agarose gel. Plasmids miniprep were done for selected colonies using EZNA Plasmid DNA Mini Kit II (Omega, D6945-02) following manufacturer's protocol and cargo-sequence were verified by DNA sequencing. List of primers used for cargo cloning could be found in appendix III.

***Creation of Cargo pWH1520* shuttles*:** 5 µg of each Cargo-TOPO shuttle and pWH1520* plasmids were restriction double digested using AvrII/BamHI (NEB) and AvrII/SpeI (NEB), following the manufacturer's protocol. Fragments of appropriate size were gel purified using 0.5% Agarose gel and the DNA bands were visualized using Crystal violet stain. DNA fragments were extracted from the excised gel band using EZNA Gel Extraction Kit (Omega, D2500-01). Digested vector pWH1520* and cargo fragments were ligated together using T4-DNA ligase (NEB) following manufacturer's protocol. The ligation mixture was transformed same as mentioned for cargo-topo shuttle preparation step. Ampicillin (100 mg/ml) containing LB-Agar plates were used for selection of colonies. Colonies carrying right constructs were identified by cPCR and restriction endonuclease digestion of miniprep plasmids from the selected colonies.

***Creation of Cargo-TcdA construct*:** Cargo-pWH1520* and pSK10401 plasmids were digested with BamHI/SphI (NEB), following manufacturer's protocol. Digested band of the desired size were analyzed and extracted as mentioned above. Desired bands obtained from pSK10401 and Cargo-pWH1520* digestions were ligated together using T4-DNA ligase and transformed by electroporation into TOP-10 *E. coli* electrocompetent cells, as mentioned previously. Selection of colonies was made using Chloramphenicol (34 mg/ml) LB-Agar plates. Plasmids from selected colonies, verified by cPCR and restriction endonuclease digestion of miniprep plasmids, were sequence verified to identify the correct clone.

***Transformation of Cargo-TcdA/Cargo-TcdA-RBD into B. megaterium*:** 200 µL of *B. megaterium* protoplast was thawed on ice followed by addition of 0.5–1.0 µg of plasmid DNA and 600 µL PEG-P (40% (w/v) PEG6000, 500 mM sucrose, 20 mM sodium malenieate, 20 mM $MgCl_2$, at pH 6.5) and mixed gently. The mixture was incubated on ice for 2–3 min before transferring it to 15.0 ml conical centrifuge tube and bringing it to the room temperature. 2.0 ml SMMP added

and mixed by gentle swirling and cells were harvested (spin at 2000 g, for 10.0 min at 25 °C). Supernatant was removed carefully without disturbing the pellet and 500.0 µL of SMMP was added before incubating the protoplast suspension 100 rpm, at 37 °C for 90–120 min. 1.5 ml of melted Top-Agar (42 °C) was then added to the protoplast suspension and the total volume of the mixture was spread over two LB-Agar plates with Tetracycline (10 mg/ml). Individual colonies were obtained after 16–24 hours were re-streaked on fresh Tetracycline containing LB-Agar plates. Colonies from the re-streaked plates were used for expression of chimeric proteins.

***Expression and purification of Cargo-TcdA/Cargo-TcdA-RBD*:** Single colony of chimera plasmid containing *B. megaterium* were grown overnight (16–20 h, 37 °C, at 200 rpm) in 5.0 ml LB containing Tetracycline (10 µg/µl), which were used to inoculate 1l of fresh LB-Tetracycline (10 mg/ml) media and incubated (37 °C, 200 rpm) until OD_{600} of 0.4–0.5 have been reached. Expression was induced by adding 10.0 ml of 50.0% of D-xylose and incubation continued for further 5–6 hours. Cells were harvested (7,000–10,000 g, 10–15 min, 4 °C) and pellet were stored at -80 °C until ready to do the purification. Cells pellet were thawed on ice then lysis buffer (50.0 mM Na_2HPO_4, 300.0 mM NaCl, 10.0 mM imidazole, pH 8.0) was added to bring the volume to 50.0 ml followed by addition of half a tablet of EDTA-free protease inhibitors cocktail tablet (ROCHE, cOmplete from Sigma - 11697498001). Suspended cell were lysed by sonication (4–6 cycles of 30 s pulse 1 min pause, 37% amplitude), and centrifuged (15,000 rpm, 4 °C, 45 min using JA-17 rotor) to obtain clear suspension. Supernatant was collected after filtering it through and 0.8 micron and then 0.2 micron syringe filters. Crude lysate was loaded on a 1.0 ml Ni affinity column pre-equilibrated with lysis buffer. Column was then washed with 10 column volume of wash buffer (50.0 mM Na_2HPO_4, 300.0 mM NaCl, 50.0 mM imidazole, pH 8.0) and protein was eluted out using 10 column volume of elution buffer (50.0 mM Na_2HPO_4, 300.0 mM NaCl, 250.0 mM

imidazole, pH 8.0). The elution fractions of 1.0 ml each were collected and analyzed on SDS-PAGE gel for the presence of protein. The column was then stripped using 10 column volume of stripping buffer (50.0 mM Na_2HPO_4, 300.0 mM NaCl, 50.0 mM EDTA, pH 8.0), then washed with 10–15 column volume of sterile water and column was stored in 20% ethanol. First 3.0 ml of elution fractions were passed through a size-exclusion chromatography (SEC) column (Superdex S-200) pre-equilibrated with lysis buffer. Lysis buffer was used to elute the protein of the SEC column attached to Bio-Rad NGC FPLC system. In case if protein were obtained from the FPLC run, a second Ni affinity column like 1st Ni column mentioned was proposed to concentrate the protein. The second Ni column however would avoid both the wash steps.

All the protein purification process, from thawing the cells to the final second Niaffinity column, were performed at 4 °C. All the work related to *B. megaterium* were done in bio-safety level- 2 (BSL-2) room. The supernatant used for protein purification, Ni affinity column steps and the SEC were done in either cold room or the cold cabinet where NGC system is in, was taken out of the BSL-2 room only after the filtration step. Analysis were done using SDS-PAGE gel analysis (4% stacking and 10–12% separation gel, 1X SDS buffer, 165 V, 4 h), stained with Coomassie stain.

***Western blot analysis*:** Two identical SDS-PAGE (4% stacking, 8% separation gel) gel loaded with protein markers, TcdA as control protein and aliquots of Cargo-TcdA/Cargo-TcdA-RBD as samples were ran (165 V, 4, 1X SDS-PAGE buffer). One gel was stained with Coomassie stain while other gel was used for western blot purpose. After removal of stacking gel the remaining piece was first washed (3X, with gentle shaking for 5 min each) with MilliQ water. Gel piece was then soaked briefly (~5 min) in transfer buffer **(**25 mM Tris 250 mM glycine, 20% methanol**)**, a piece of polyvinylidene (PVDF) membrane of the size of gel piece was cut and soaked in methanol

for 3–5 min. The gel piece was placed on the PVDF membrane and sandwiched between pieces of filter papers (3 on either side) presoaked in transfer buffer. The electrophoresis equipment was set up for the protein transfer from the gel to PVDF membrane and electrophoresis was ran using transfer buffer at low temperature for prolonged period (4 °C, 100 V, 12 hr). Once the transfer is done the PVDF membrane was washed with MilliQ water (3X wash with gentle shaking, 5 min each) followed by, developing the film for visualization using rabbit anti-His-6 primary and goat anti-rabbit horseradish peroxidase conjugated secondary antibodies following the manufacturer's protocol. The PVDF film after transfer step was developed using HRP-substrate (Thermo-Pierce, 32106) following the manufacturer's protocol.

***B. Megaterium codon bias analysis*:** Kazusa Codon Usage Database (http://www.kazusa.or.jp/codon) has been used to compare the codon usage of *B. megaterium* against the eukaryotic origin proteins (cargos and RBDs) as well as TcdA. The usage of all possible codons for every amino acid were compared between *B. megaterium* and the proteins mentioned. A codon for an amino acid which has been used <10% among all the codons for that amino acid has been termed as problem codon. Differential codon usage was calculated (codon usage in *B. megaterium* - codon usage of the protein of interest; done by Adam Boyden).

Appendix I: List of plasmid constructs prepared for DEAD-box helicasess project

Plasmid code	Parent plasmid	Sequence verified	Comments
pAU01011	pET28a	yes	carrys C-terminal His6-tagged RhlB.
pAU01012	pUC19	yes	carrys hns (-30 to +60) sequence with T7 RNAP promoter sequence for in vitro transcription
pAU01013	pUC19	yes	carrys ompC (-81 to + 60) sequence with T7 RNAP promoter sequence for in vitro transcription
pAU01014	pUC19	yes	carrys ompF (-110 to +60) sequence with T7 RNAP promoter sequence for in vitro transcription
pAU01015	pUC19	yes	carrys sdhC (-220 to +60) sequence with T7 RNAP promoter sequence for in vitro transcription
pAU01016	pUC19	yes	carrys glmS (-143 to +60) sequence with T7 RNAP promoter sequence for in vitro transcription
pAU01017	pUC19	yes	carrys full length glmZ sequence with T7 RNAP promoter sequence for in vitro transcription
pAU01018	pUC19	yes	carrys full length glmY sequence with T7 RNAP promoter sequence for in vitro transcription
pAU01019	pUC19	yes	carrys fulllength ryhB sequence with T7 RNAP promoter sequence for in vitro transcription
pAU01020	pUC19	yes	carrys full length rybB sequence with T7 RNAP promoter sequence for in vitro transcription

Plasmid constructs prepared for the DEAD-box helicases project.

Appendix II: List of chimeric constructs

Construct	Abbreviation
Bax*-TcdA-CROP	BAC
Bax2-TcdA-CROP	B2AC
Bax*-TcdA-EGF	BAE
Bax*-TcdA-VEGF	BAV
XIAP-TcdA-CROP	XAC
XIAP-TcdA-EGF	XAE
XIAP-TcdA-VEGF	XAV
XIAP-TcdA-BoNT	XAB
Casp9-TcdA-EGF	CAE
Casp9-TcdA-CROP	CAC

Complete chimeric constructs with abbreviations

Appendix III: List of chimera subcloning primers

Primers number	Primers name	Prmers sequence	Polymer-ase used	Annealing temp used(°C)	Elongati-on time (min)	Restricti-on site
1	Bax-for	5'- GTC CAA CCT AGG AGA TCT ATG GAC GGG TCC GGG GAG C -3'	Pfu	65	3	AvrII
2	Bax-rev	5'- AGA AAG GGA TCC CGC CAG TTT ACT AGC AAT AAA TTC AAG AGA ATC CAA CAC GCC CAT CTT CTT CCA GAT GGT GAG TGA GG -3'	Pfu	65	3	BamHI
3	Bax-BamHI-SDM-for	5'- GCG GCT GTT GGG CTG GAT TCA AGA CCA GGG TGG TTG G -3'	Pfu	65	12	**
4	Bax-BamHI-SDM-rev	5'- CCA ACC ACC CTG GTC TTG AAT CCA GCC CAA CAG CCG C -3'	Pfu	65	12	**
5	Casp9-for	5'- GTC CAA CCT AGG AGA TCT ATG GAC GAA GCG GAT CGG C -3'	Pfu	65	4	AvrII
6	Casp9-rev	5'- AGA AAG GGA TCC CGC CAG TTT ACT AGC AAT AAA TTC AAG AGA ATC CAA CAC TGA TGT TTT AAA GAA AAG TTT TTT CCG GAG G -3'	Pfu	65	4	BamHI
7	p35-for	5'- GTC CAA CCT AGG AGA TCT ATG GGC ACG GTG CTG TCC C -3'	Pfu	65	3	AvrII
8	p-35-rev	5'- AGA AAG GGA TCC CGC CAGT TTA CTA GCA ATA AAT TCA AGA GAA TCC AAC ACC CGA TCC AGG CCT AGG AGG AGC C -3'	Pfu	65	3	BamHI
9	p35-AvrII-SDM-for	5'- GGA CAA GAA GCG GCT CCT CCT GGG CCT GGA TCG GGT GTT GG -3'	Pfu	65	12	**
10	p35-AvrII-SDM-rev	5'- CCA ACA CCC GAT CCA GGC CCA GGA GGA GCC GCT TCT TGT CC -3'	Pfu	65	12	**
11	XIAP-for	5'- GTC CAA CCT AGG AGA TCT ATG ACT TTT AAC AGT TTT GAA GGA TCT AAA ACT TGT GTA CCT GC -3'	Pfu	65	4	AvrII
12	XIAP-rev	5'- AGA AAG GGA TCC CGC CAG TTT ACT AGC AAT AAA TTC AAG AGA ATC CAA CAC AGA CAT AAA AAT TTT TTG CTT GAA AGT AAT GAC TGT GTA GCA C -3'	Pfu	65	4	BamHI

Chimera subcloning primers for cargo subcloning to TOPO-plasmid. **Bax-BamHI-SDM and p35-AvrII-SDM primers were used to mutate the BamHI and AvrII restriction sites present in the coding sequence of Bax and p35 gene respectively. SDM pcr were run using the Bax and p35 coding sequence carrying TOPO plasmids.

Appendix IV: List of chimera sequencing primers

Primers number	Primers name	Primers sequence
1	M13-F	5'- CAG GAA ACA GCT ATG AC -3'
2	M13-R	5'- GTA AAA CGA CGC CAG T -3'
3	W5	5'- GTT GAT GGA TAA ACT TGT TC -3'
4	W3	5'- CAT CCA GCC TCG CGT C -3'
5	TcdA-2326-R	5'- CGC TTG TGT TGA ATT CAT C -3'
6	TcdA-2326-F	5'- GAT GAA TTC AAC ACA ACG C -3'
7	TcdA-3065-F	5'- CAA AAG TAA TGG TGA GTC -3'
8	TcdA-3727-F	5'- CTA TTT TAA TCA TTT GTC TG -3'
9	TcdA-4258-F	5'- GCC AAC TAT AAC TAC TAA C -3'
10	TcdA-4502-F	5'- CTT ATT ATA GGC AAT CAA C -3'
11	TcdA-5034-F	5'- CCG TAT ACT CAT CTT ACC -3'
12	TcdA-5268-F	5'- CAT CGT CAT CTA AAA GCA C -3'
13	TcdA-5720-F	5'- TCA TTA GGA TAT ATA ATG AG -3'
14	Casp9-int-seq-F	5'- GAA CTT CTG CCG TGA GTC C -3'
15	Casp9-int-seq-R	5'- GCC AGC ACC ATT TTC TTG -3'
16	XIAP-int-seq-F	5'- GCG ACA CTT TCC TAA TTG C -3'
17	XIAP-int-seq-R	5'- AAT CCA GCT CTT GCA AGC -3'
18	Cargo-seq-For	5'- ATG ATG AGA TAA AGT TAG TTT ATT GG -3'
19	Cargo-seq-Rev	5'- GTA TGA TAT AAT GAA CAT AAT TTT TAC TTC C -3'
20	RBD-seq-For	5'- GAA AAT GAA TTA GAT AGA GAT CAT TTA GG -3'
21	RBD-seq-Rev	5'- GAA GCG AGA AGA ATC ATA ATG G -3'

List of sequencing primers used to sequence the cargo and the RBD shuttle vectors and, the prepared protein chimera clones.

References

1. Huang, H. Y.; Chang, H. Y.; Chou, C. H.; Tseng, C. P.; Ho, S. Y.; Yang, C. D.; Ju, Y. W.; Huang, H. D., sRNAMap: genomic maps for small non-coding RNAs, their regulators and their targets in microbial genomes. *Nucleic Acids Res* **2009,** *37* (Database issue), D150-4.
2. Raghavan R., G. E. A., Ochman H., Genome-wide detection of novel regulatory RNAs in E. coli. *Genome Research* **2011,** *21*, 1487-1497.
3. Lalaouna D., C. M., Semsey S., Brouard JS., Wang J., Wade J. T., Masse E., A 3' external transcribed spacer in a tRNA transcript acts as a sponge for small RNAs to prevent transcriptional noise. *Molecular Cell* **2015,** *58*, 393-405.
4. Philippe B., F. R., Fresh layers of RNA-mediated regulation in Gram-positive bacteria. *Current Opinion in Microbiology* **2016,** *30*, 30-35.
5. Lay N. R. De. , G. D. A., The unmasking of 'junk' RNA reveals novel sRNAs: from processed RNA fragments to marooned riboswitches. *Current Opinion in Microbiology* **2016,** *30*, 16-21.
6. Wadler C. S., V. C. K., A dual function for a bacterial small RNA: SgrS performs base pairing-dependent regulation and encodes a functional polypeptide. *Proceedings of the National Academy of Sciences of the United States of America* **2007,** *104* (51), 20454-20459.
7. Gimpel M., H. N., Mäder U., Krügel H., Brantl S., A dual-function sRNA from B. subtilis: SR1 acts as a peptide encoding mRNA on the gapA operon. *Molecular Microbiology* **2010,** *76* (4), 990-1009.

8. Novick R. P., R. H. F., Projan S. J., Kornblum J., Kreiswirth B., Moghazeh S, Synthesis of staphylococcal virulence factors is controlled by a regulatory RNA molecule. *The EMBO Journal* **1993,** *12* (10), 3967-3975.

9. Chao, Y., Papenfort, K., Reinhardt, R., Sharma, C. M., Vogel, J., An atlas of Hfq-bound transcripts reveals 3′ UTRs as a genomic reservoir of regulatory small RNAs. *The EMBO journal* **2012,** *31* (20), 4005-4019.

10. Vogel, J., Bartels, V., Tang, T. H., Churakov, G., Slagter-Jäger, J. G., Hüttenhofer, A., & Wagner, E. G. H., RNomics in Escherichia coli detects new sRNA species and indicates parallel transcriptional output in bacteria. *Nucleic acids research* **2003,** *31* (22), 6435-6443.

11. Kim, H. M., Shin, J. H., Cho, Y. B., Roe, J. H. , Inverse regulation of Fe-and Ni-containing SOD genes by a Fur family regulator Nur through small RNA processed from 3′ UTR of the sodF mRNA. *Nucleic Acids Research* **2014,** *42* (3), 2003-2014.

12. Figueroa-Bossi, N., Valentini, M., Malleret, L., Bossi, L., Caught at its own game: regulatory small RNA inactivated by an inducible transcript mimicking its target. *Genes & development* **2009,** *23* (17), 2004-2015.

13. Miyakoshi, M., Chao, Y., Vogel, J. , Cross talk between ABC transporter mRNAs via a target mRNA-derived sponge of the GcvB small RNA. *The EMBO journal* **2015**, 1478-1492.

14. Loh, E., Dussurget, O., Gripenland, J., Vaitkevicius, K., Tiensuu, T., Mandin, P., ... & Johansson, J., Repoila F., Buchrieser C., Cossart P., Johansson J., A trans-acting riboswitch controls expression of the virulence regulator PrfA in Listeria monocytogenes. *Cell* **2009,** *139* (4), 770-779.

15. Wagner E. G. H., R. P., *Small RNAs in Bacteria and Archaea: Who They Are, What They Do, and How They Do It*. 1st ed.; Elsevier: 2016; Vol. 90.

16. Kumar, P., Anaya, J., Mudunuri, S. B., Dutta, A., Meta-analysis of tRNA derived RNA fragments reveals that they are evolutionarily conserved and associate with AGO proteins to recognize specific RNA targets. *BMC biology* **2014,** *12* (1), 78.

17. Lee, Y. S., Shibata, Y., Malhotra, A., Dutta, A., A novel class of small RNAs: tRNA-derived RNA fragments (tRFs). *Genes & development* **2009,** *23* (22), 2639-2649.

18. Brantl, S., Bacterial gene regulation: from transcription attenuation to riboswitches and ribozymes. *Trends in microbiology* **2004,** *12* (11), 473-475.

19. Breaker, R. R., Prospects for riboswitch discovery and analysis. *Molecular cell* **2011,** *43* (6), 867-879.

20. Andre, G., Even, S., Putzer, H., Burguiere, P., Croux, C., Danchin, A., Martin-Verstraete I., Soutourina, O., S-box and T-box riboswitches and antisense RNA control a sulfur metabolic operon of Clostridium acetobutylicum. *Nucleic acids research* **2008,** *36* (18), 5955-5969.

21. Mellin, J. R., Tiensuu, T., Bécavin, C., Gouin, E., Johansson, J., & Cossart, P., A riboswitch-regulated antisense RNA in Listeria monocytogenes. *Proceedings of the National Academy of Sciences of the United States of America* **2013,** *110* (32), 13132-13137.

22. Chen, J., Gottesman, S., Riboswitch regulates RNA. *Science* **2014,** *345* (6199), 876-877.

23. DebRoy, S., Gebbie, M., Ramesh, A., Goodson, J. R., Cruz, M. R., van Hoof, A., Winkler W. C., Garsin, D. A., A riboswitch-containing sRNA controls gene expression by sequestration of a response regulator. *Science* **2014,** *345* (6199), 937-940.

24. Mellin, J. R., Koutero, M., Dar, D., Nahori, M. A., Sorek, R., Cossart, P., 940-943., Sequestration of a two-component response regulator by a riboswitch-regulated noncoding RNA. *Science* **2014,** *345* (6199), 940-943.

25. Georg, J., Hess, W. R. , cis-antisense RNA, another level of gene regulation in bacteria. *Microbiology and Molecular Biology Reviews* **2011,** *75* (2), 286-300.

26. Storz G., V. J., Wassarman K. M., Regulation by Small RNAs in Bacteria: Expanding Frontiers. *Molecular Cell* **2011,** *43* (6), 880-891.

27. Papenfort, K., Vogel, J. , Regulatory RNA in bacterial pathogens. Cell host & microbe. *Cell host & microbe* **2010,** *8* (1), 116-127.

28. Updegrove, T. B., Zhang, A., Storz, G., Hfq: the flexible RNA matchmaker. *Current opinion in microbiology* **2016,** *30*, 133-138.

29. Cech, G. M.; Szalewska-Palasz, A.; Kubiak, K.; Malabirade, A.; Grange, W.; Arluison, V.; Wegrzyn, G., The Escherichia Coli Hfq Protein: An Unattended DNA-Transactions Regulator. *Frontiers in molecular biosciences* **2016,** *3*, 36.

30. Feliciano, J. R.; Grilo, A. M.; Guerreiro, S. I.; Sousa, S. A.; Leitao, J. H., Hfq: a multifaceted RNA chaperone involved in virulence. *Future microbiology* **2016,** *11* (1), 137-51.

31. Murina, V. N.; Nikulin, A. D., Bacterial Small Regulatory RNAs and Hfq Protein. *Biochemistry. Biokhimiia* **2015,** *80* (13), 1647-54.

32. Obregon, K. A.; Hoch, C. T.; Sukhodolets, M. V., Sm-like protein Hfq: Composition of the native complex, modifications, and interactions. *Biochimica et biophysica acta* **2015,** *1854* (8), 950-66.

33. Gottesman, S.; Storz, G., RNA reflections: converging on Hfq. *Rna* **2015,** *21* (4), 511-2.

34. Butland, G.; Peregrín-Alvarez, J. M.; Li, J.; Yang, W.; Yang, X.; Canadien, V.; Starostine, A.; Richards, D.; Beattie, B.; Krogan, N., Interaction network containing conserved and essential protein complexes in Escherichia coli. *Nature* **2005,** *433* (7025), 531-537.

35. Holmqvist, E.; Wright, P. R.; Li, L.; Bischler, T.; Barquist, L.; Reinhardt, R.; Backofen, R.; Vogel, J., Global RNA recognition patterns of post-transcriptional regulators Hfq and CsrA revealed by UV crosslinking in vivo. *Embo j* **2016,** *35* (9), 991-1011.

36. Attaiech, L.; Glover, J. M.; Charpentier, X., RNA Chaperones Step Out of Hfq's Shadow. *Trends in Microbiology* **2017**.

37. Attaiech, L.; Boughammoura, A.; Brochier-Armanet, C.; Allatif, O.; Peillard-Fiorente, F.; Edwards, R. A.; Omar, A. R.; MacMillan, A. M.; Glover, M.; Charpentier, X., Silencing of natural transformation by an RNA chaperone and a multitarget small RNA. *Proceedings of the National Academy of Sciences* **2016,** *113* (31), 8813-8818.

38. Franze de Fernandez, M.; Eoyang, L.; August, T., Factor fraction required for the synthesis of bacteriophage Qβ-RNA. *Nature* **1968,** *219* (5154), 588-590.

39. Sobrero, P., & Valverde, C., The bacterial protein Hfq: much more than a mere RNA-binding factor. *Critical reviews in microbiology* **2012,** *38* (4), 276-299.

40. Vogel, J., Luisi, B. F., Hfq and its constellation of RNA. *Nature Reviews Microbiology* **2011,** *9* (8), 578-589.

41. Lee, T., Feig, A. L., *The RNA–protein complexes of E. coli Hfq: form and function*. Springer Berlin Heidelberg.: 2009.

42. Muffler, A.; Traulsen, D. D.; Fischer, D.; Lange, R.; Hengge-Aronis, R., The RNA-binding protein HF-I plays a global regulatory role which is largely, but not exclusively, due to its

role in expression of the sigmaS subunit of RNA polymerase in Escherichia coli. *Journal of bacteriology* **1997,** *179* (1), 297-300.

43. Link, T. M.; Valentin-Hansen, P.; Brennan, R. G., Structure of Escherichia coli Hfq bound to polyriboadenylate RNA. *Proceedings of the National Academy of Sciences* **2009,** *106* (46), 19292-19297.

44. Mikulecky, P. J.; Kaw, M. K.; Brescia, C. C.; Takach, J. C.; Sledjeski, D. D.; Feig, A. L., Escherichia coli Hfq has distinct interaction surfaces for DsrA, rpoS and poly (A) RNAs. *Nature structural & molecular biology* **2004,** *11* (12), 1206-1214.

45. Schumacher, M. A.; Pearson, R. F.; Møller, T.; Valentin-Hansen, P.; Brennan, R. G., Structures of the pleiotropic translational regulator Hfq and an Hfq–RNA complex: a bacterial Sm-like protein. *The EMBO journal* **2002,** *21* (13), 3546-3556.

46. Salim, N. N.; Feig, A. L., An upstream Hfq binding site in the fhlA mRNA leader region facilitates the OxyS-fhlA interaction. *PLoS One* **2010,** *5* (9), e13028.

47. Panja, S.; Santiago-Frangos, A.; Schu, D. J.; Gottesman, S.; Woodson, S. A., Acidic Residues in the Hfq Chaperone Increase the Selectivity of sRNA Binding and Annealing. *J Mol Biol* **2015,** *427* (22), 3491-500.

48. Zheng, A.; Panja, S.; Woodson, S. A., Arginine Patch Predicts the RNA Annealing Activity of Hfq from Gram-Negative and Gram-Positive Bacteria. *J Mol Biol* **2016,** *428* (11), 2259-64.

49. Schu, D. J.; Zhang, A.; Gottesman, S.; Storz, G., Alternative Hfq-sRNA interaction modes dictate alternative mRNA recognition. *Embo j* **2015,** *34* (20), 2557-73.

50. Večerek, B.; Rajkowitsch, L.; Sonnleitner, E.; Schroeder, R.; Bläsi, U., The C-terminal domain of Escherichia coli Hfq is required for regulation. *Nucleic acids research* **2008,** *36* (1), 133-143.

51. Cho, C.; Lee, S. Y., Efficient gene knockdown in Clostridium acetobutylicum by synthetic small regulatory RNAs. *Biotechnol Bioeng* **2017,** *114* (2), 374-383.

52. Caillet, J.; Gracia, C.; Fontaine, F.; Hajnsdorf, E., Clostridium difficile Hfq can replace Escherichia coli Hfq for most of its function. *Rna* **2014,** *20* (10), 1567-78.

53. Santiago-Frangos, A.; Kavita, K.; Schu, D. J.; Gottesman, S.; Woodson, S. A., C-terminal domain of the RNA chaperone Hfq drives sRNA competition and release of target RNA. *Proceedings of the National Academy of Sciences* **2016**, 201613053.

54. Windbichler, N.; von Pelchrzim, F.; Mayer, O.; Csaszar, E.; Schroeder, R., Isolation of small RNA-binding proteins from E. coli: evidence for frequent interaction of RNAs with RNA polymerase. *RNA biology* **2008,** *5* (1), 30-40.

55. Sukhodolets, M. V.; Garges, S., Interaction of Escherichia coli RNA polymerase with the ribosomal protein S1 and the Sm-like ATPase Hfq. *Biochemistry* **2003,** *42* (26), 8022-8034.

56. Morita, T.; Maki, K.; Aiba, H., RNase E-based ribonucleoprotein complexes: mechanical basis of mRNA destabilization mediated by bacterial noncoding RNAs. *Genes & development* **2005,** *19* (18), 2176-2186.

57. Morita, T.; Aiba, H., RNase E action at a distance: degradation of target mRNAs mediated by an Hfq-binding small RNA in bacteria. *Genes & development* **2011,** *25* (4), 294-298.

58. Ikeda, Y.; Yagi, M.; Morita, T.; Aiba, H., Hfq binding at RhlB-recognition region of RNase E is crucial for the rapid degradation of target mRNAs mediated by sRNAs in Escherichia coli. *Molecular microbiology* **2011,** *79* (2), 419-432.

59. Chao, Y.; Li, L.; Girodat, D.; Förstner, K. U.; Said, N.; Corcoran, C.; Śmiga, M.; Papenfort, K.; Reinhardt, R.; Wieden, H.-J., In Vivo Cleavage Map Illuminates the Central Role of RNase E in Coding and Non-coding RNA Pathways. *Molecular Cell* **2017,** *65* (1), 39-51.

60. Carpousis, A. J., The RNA degradosome of Escherichia coli: an mRNA-degrading machine assembled on RNase E. *Annu. Rev. Microbiol.* **2007,** *61*, 71-87.

61. Mohanty, B. K.; Maples, V. F.; Kushner, S. R., The Sm-like protein Hfq regulates polyadenylation dependent mRNA decay in Escherichia coli. *Molecular microbiology* **2004,** *54* (4), 905-920.

62. De Lay, N.; Gottesman, S., RNase E Finds Some sRNAs Stimulating. *Molecular cell* **2012,** *47* (6), 825-826.

63. Bandyra, K. J.; Said, N.; Pfeiffer, V.; Górna, M. W.; Vogel, J.; Luisi, B. F., The seed region of a small RNA drives the controlled destruction of the target mRNA by the endoribonuclease RNase E. *Molecular cell* **2012,** *47* (6), 943-953.

64. Rabhi, M.; Espéli, O.; Schwartz, A.; Cayrol, B.; Rahmouni, A. R.; Arluison, V.; Boudvillain, M., The Sm-like RNA chaperone Hfq mediates transcription antitermination at Rho-dependent terminators. *The EMBO journal* **2011,** *30* (14), 2805-2816.

65. Moreno, R.; Martínez-Gomariz, M.; Yuste, L.; Gil, C.; Rojo, F., The Pseudomonas putida Crc global regulator controls the hierarchical assimilation of amino acids in a complete medium: evidence from proteomic and genomic analyses. *Proteomics* **2009,** *9* (11), 2910-2928.

66. Rojo, F., Carbon catabolite repression in Pseudomonas: optimizing metabolic versatility and interactions with the environment. *FEMS microbiology reviews* **2010,** *34* (5), 658-684.

67. Görke, B.; Stülke, J., Carbon catabolite repression in bacteria: many ways to make the most out of nutrients. *Nature Reviews Microbiology* **2008,** *6* (8), 613-624.

68. Moreno, R.; Marzi, S.; Romby, P.; Rojo, F., The Crc global regulator binds to an unpaired A-rich motif at the Pseudomonas putida alkS mRNA coding sequence and inhibits translation initiation. *Nucleic acids research* **2009,** *37* (22), 7678-7690.

69. Sonnleitner, E.; Abdou, L.; Haas, D., Small RNA as global regulator of carbon catabolite repression in Pseudomonas aeruginosa. *Proceedings of the National Academy of Sciences* **2009,** *106* (51), 21866-21871.

70. Sonnleitner, E.; Valentini, M.; Wenner, N.; el Zahar Haichar, F.; Haas, D.; Lapouge, K., Novel targets of the CbrAB/Crc carbon catabolite control system revealed by transcript abundance in Pseudomonas aeruginosa. *PloS one* **2012,** *7* (10), e44637.

71. Hernández-Arranz, S.; Sánchez-Hevia, D.; Rojo, F.; Moreno, R., Effect of Crc and Hfq proteins on the transcription, processing, and stability of the Pseudomonas putida CrcZ sRNA. *RNA* **2016,** *22* (12), 1902-1917.

72. Moreno, R.; Hernández-Arranz, S.; La Rosa, R.; Yuste, L.; Madhushani, A.; Shingler, V.; Rojo, F., The Crc and Hfq proteins of Pseudomonas putida cooperate in catabolite repression and formation of ribonucleic acid complexes with specific target motifs. *Environmental microbiology* **2015,** *17* (1), 105-118.

73. Inaoka, T.; Ochi, K., RelA protein is involved in induction of genetic competence in certain Bacillus subtilis strains by moderating the level of intracellular GTP. *Journal of bacteriology* **2002,** *184* (14), 3923-3930.

74. Metzger, S.; Sarubbi, E.; Glaser, G.; Cashel, M., Protein sequences encoded by the relA and the spoT genes of Escherichia coli are interrelated. *Journal of Biological Chemistry* **1989,** *264* (16), 9122-9125.

75. Metzger, S.; Schreiber, G.; Aizenman, E.; Cashel, M.; Glaser, G., Characterization of the relA1 mutation and a comparison of relA1 with new relA null alleles in Escherichia coli. *Journal of Biological Chemistry* **1989,** *264* (35), 21146-21152.

76. Potrykus, K.; Cashel, M., (p) ppGpp: still Magical? *Annu. Rev. Microbiol.* **2008,** *62*, 35-51.

77. Argaman, L.; Elgrably-Weiss, M.; Hershko, T.; Vogel, J.; Altuvia, S., RelA protein stimulates the activity of RyhB small RNA by acting on RNA-binding protein Hfq. *Proceedings of the National Academy of Sciences* **2012,** *109* (12), 4621-4626.

78. Davies, B. W.; Köhrer, C.; Jacob, A. I.; Simmons, L. A.; Zhu, J.; Aleman, L. M.; RajBhandary, U. L.; Walker, G. C., Role of Escherichia coli YbeY, a highly conserved protein, in rRNA processing. *Molecular microbiology* **2010,** *78* (2), 506-518.

79. Jacob, A. I.; Köhrer, C.; Davies, B. W.; RajBhandary, U. L.; Walker, G. C., Conserved bacterial RNase YbeY plays key roles in 70S ribosome quality control and 16S rRNA maturation. *Molecular cell* **2013,** *49* (3), 427-438.

80. Warner, J. R., YbeY: the jealous tailor. *Molecular cell* **2013,** *49* (3), 422-423.

81. Rasouly, A.; Ron, E. Z., Interplay between the heat shock response and translation in Escherichia coli. *Research in microbiology* **2009,** *160* (4), 288-296.

82. Pandey, S. P.; Minesinger, B. K.; Kumar, J.; Walker, G. C., A highly conserved protein of unknown function in Sinorhizobium meliloti affects sRNA regulation similar to Hfq. *Nucleic acids research* **2011**, gkr060.

83. Pandey, S. P.; Winkler, J. A.; Li, H.; Camacho, D. M.; Collins, J. J.; Walker, G. C., Central role for RNase YbeY in Hfq-dependent and Hfq-independent small-RNA regulation in bacteria. *BMC genomics* **2014,** *15* (1), 121.

84. G. Chaulk, S.; Smith− Frieday, M. N.; Arthur, D. C.; Culham, D. E.; Edwards, R. A.; Soo, P.; Frost, L. S.; Keates, R. A.; Glover, J. M.; Wood, J. M., ProQ is an RNA chaperone that controls ProP levels in Escherichia coli. *Biochemistry* **2011,** *50* (15), 3095-3106.

85. Smith, M. N.; Crane, R. A.; Keates, R. A.; Wood, J. M., Overexpression, purification, and characterization of ProQ, a posttranslational regulator for osmoregulatory transporter ProP of Escherichia coli. *Biochemistry* **2004,** *43* (41), 12979-12989.

86. Smith, M. N.; Kwok, S. C.; Hodges, R. S.; Wood, J. M., Structural and functional analysis of ProQ: an osmoregulatory protein of Escherichia coli. *Biochemistry* **2007,** *46* (11), 3084-3095.

87. Attar, N., Bacterial physiology: A new chaperone for regulatory sRNAs. *Nature Reviews Microbiology* **2016,** *14* (11), 664-665.

88. Timmermans, J.; Van Melderen, L., Post-transcriptional global regulation by CsrA in bacteria. *Cellular and molecular life sciences* **2010,** *67* (17), 2897-2908.

89. Romeo, T., Global regulation by the small RNA-binding protein CsrA and the non-coding RNA molecule CsrB. *Molecular microbiology* **1998,** *29* (6), 1321-1330.

90. DUBEY, A. K.; BAKER, C. S.; ROMEO, T.; BABITZKE, P., RNA sequence and secondary structure participate in high-affinity CsrA–RNA interaction. *Rna* **2005,** *11* (10), 1579-1587.

91. Liu, M. Y.; Gui, G.; Wei, B.; Preston, J. F.; Oakford, L.; Yüksel, Ü.; Giedroc, D. P.; Romeo, T., The RNA molecule CsrB binds to the global regulatory protein CsrA and

antagonizes its activity in Escherichia coli. *Journal of Biological Chemistry* **1997,** *272* (28), 17502-17510.

92. Holmqvist, E.; Vogel, J., A small RNA serving both the Hfq and CsrA regulons. *Genes & development* **2013,** *27* (10), 1073-1078.

93. Kulkarni, P. R.; Cui, X.; Williams, J. W.; Stevens, A. M.; Kulkarni, R. V., Prediction of CsrA-regulating small RNAs in bacteria and their experimental verification in Vibrio fischeri. *Nucleic acids research* **2006,** *34* (11), 3361-3369.

94. Linder, P., Birth of the DEAD box. *Nature* **1989,** *337*, 121-122.

95. Linder, P., Dead-box proteins: a family affair—active and passive players in RNP-remodeling. *Nucleic acids research* **2006,** *34* (15), 4168–4180.

96. Jankowsky, E.; Fairman, M. E., RNA helicases—one fold for many functions. *Current opinion in structural biology* **2007,** *17* (3), 316–324.

97. Ambrus, A. M.; Frolov, M. V., The diverse roles of RNA helicases in RNAi. *Cell Cycle* **2009,** *8* (21), 3500–3505.

98. Martin, R.; Straub, A. U.; Doebele, C.; Bohnsack, M. T., DExD/H-box RNA helicases in ribosome biogenesis. *RNA biology* **2013,** *10* (1), 4–18.

99. Owttrim, G. W., RNA helicases: diverse roles in prokaryotic response to abiotic stress. *RNA biology* **2013,** *10* (1), 96–110.

100. Fuller-Pace, F. V.; Moore, H. C., RNA helicases p68 and p72: multifunctional proteins with important implications for cancer development. *Future oncology* **2011,** *7* (2), 239–251.

101. Parsyan, A.; Svitkin, Y.; Shahbazian, D.; Gkogkas, C.; Lasko, P.; Merrick, W. C.; Sonenberg, N., mRNA helicases: the tacticians of translational control. *Nature reviews Molecular cell biology* **2011,** *12* (4), 235–245.

102. Fairman-Williams, M. E.; Guenther, U.-P.; Jankowsky, E., SF1 and SF2 helicases: family matters. *Current opinion in structural biology* **2010,** *20* (3), 313–324.

103. Singleton, M. R.; Dillingham, M. S.; Wigley, D. B., Structure and mechanism of helicases and nucleic acid translocases. *Annu. Rev. Biochem.* **2007,** *76*, 23–50.

104. Iost, I.; Dreyfus, M., DEAD-box RNA helicases in Escherichia coli. *Nucleic acids research* **2006,** *34* (15), 4189–4197.

105. Rössler, O. G.; Straka, A.; Stahl, H., Rearrangement of structured RNA via branch migration structures catalysed by the highly related DEAD-box proteins p68 and p72. *Nucleic Acids Research* **2001,** *29* (10), 2088–2096.

106. Huang, Y.; Liu, Z.-R., The ATPase, RNA unwinding, and RNA binding activities of recombinant p68 RNA helicase. *Journal of Biological Chemistry* **2002,** *277* (15), 12810–12815.

107. Chamot, D.; Colvin, K. R.; Kujat-Choy, S. L.; Owttrim, G. W., RNA structural rearrangement via unwinding and annealing by the cyanobacterial RNA helicase, CrhR. *Journal of Biological Chemistry* **2005,** *280* (3), 2036–2044.

108. Henn, A.; Bradley, M. J.; De La Cruz, E. M., ATP utilization and RNA conformational rearrangement by DEAD-box proteins. *Annual review of biophysics* **2012,** *41*, 247–267.

109. Jarmoskaite, I.; Russell, R., DEAD-box proteins as RNA helicases and chaperones. *Wiley Interdisciplinary Reviews: RNA* **2011,** *2* (1), 135–152.

110. Tsu, C. A.; Kossen, K.; Uhlenbeck, O. C., The Escherichia coli DEAD protein DbpA recognizes a small RNA hairpin in 23S rRNA. *Rna* **2001,** *7* (5), 702–709.

111. Fuller-Pace, F.; Nicol, S.; Reid, A.; Lane, D., DbpA: a DEAD box protein specifically activated by 23s rRNA. *The EMBO Journal* **1993,** *12* (9), 3619.

112. Diges, C. M.; Uhlenbeck, O. C., Escherichia coli DbpA is an RNA helicase that requires hairpin 92 of 23S rRNA. *The EMBO journal* **2001,** *20* (19), 5503–5512.

113. Karginov, F. V.; Caruthers, J. M.; Hu, Y.; McKay, D. B.; Uhlenbeck, O. C., YxiN is a modular protein combining a DExD/H core and a specific RNA-binding domain. *Journal of Biological Chemistry* **2005,** *280* (42), 35499–35505.

114. Grohman, J. K.; Del Campo, M.; Bhaskaran, H.; Tijerina, P.; Lambowitz, A. M.; Russell, R., Probing the mechanisms of DEAD-box proteins as general RNA chaperones: the C-terminal domain of CYT-19 mediates general recognition of RNA. *Biochemistry* **2007,** *46* (11), 3013.

115. Mohr, G.; Del Campo, M.; Mohr, S.; Yang, Q.; Jia, H.; Jankowsky, E.; Lambowitz, A. M., Function of the C-terminal domain of the DEAD-box protein Mss116p analyzed *in vivo* and *in vitro*. *Journal of molecular biology* **2008,** *375* (5), 1344–1364.

116. Yang, Q.; Del Campo, M.; Lambowitz, A. M.; Jankowsky, E., DEAD-box proteins unwind duplexes by local strand separation. *Molecular cell* **2007,** *28* (2), 253–263.

117. Tran, E. J.; Zhou, Y.; Corbett, A. H.; Wente, S. R., The DEAD-box protein Dbp5 controls mRNA export by triggering specific RNA: protein remodeling events. *Molecular cell* **2007,** *28* (5), 850–859.

118. Moore, A. F.; Gentry, R. C.; Koculi, E., DbpA is a region-specific RNA helicase. *Biopolymers* **2017**.

119. Jagessar, K. L.; Jain, C., Functional and molecular analysis of Escherichia coli strains lacking multiple DEAD-box helicases. *Rna* **2010,** *16* (7), 1386–1392.

120. Jain, C., The E. coli RhlE RNA helicase regulates the function of related RNA helicases during ribosome assembly. *Rna* **2008,** *14* (2), 381–389.

121. Resch, A.; Većerek, B.; Palavra, K.; Bläsi, U., Requirement of the CsdA DEAD-box helicase for low temperature riboregulation of rpoS mRNA. *RNA biology* **2010,** *7* (6), 796–802.

122. Taghbalout, A.; Rothfield, L., RNaseE and the other constituents of the RNA degradosome are components of the bacterial cytoskeleton. *Proceedings of the National Academy of Sciences* **2007,** *104* (5), 1667–1672.

123. Taghbalout, A.; Rothfield, L., RNaseE and RNA helicase B play central roles in the cytoskeletal organization of the RNA degradosome. *Journal of Biological Chemistry* **2008,** *283* (20), 13850–13855.

124. Py, B.; Higgins, C. F.; Krisch, H. M.; Carpousis, A. J., A DEAD-box RNA helicase in the Escherichia coli RNA degradosome. *Nature* **1996,** *381* (6578), 169.

125. Worrall, J. A.; Howe, F. S.; McKay, A. R.; Robinson, C. V.; Luisi, B. F., Allosteric activation of the ATPase activity of the Escherichia coli RhlB RNA helicase. *Journal of Biological Chemistry* **2008,** *283* (9), 5567–5576.

126. Coburn, G. A.; Miao, X.; Briant, D. J.; Mackie, G. A., Reconstitution of a minimal RNA degradosome demonstrates functional coordination between a 3′ exonuclease and a DEAD-box RNA helicase. *Genes & development* **1999,** *13* (19), 2594–2603.

127. Chandran, V.; Poljak, L.; Vanzo, N. F.; Leroy, A.; Miguel, R. N.; Fernandez-Recio, J.; Parkinson, J.; Burns, C.; Carpousis, A. J.; Luisi, B. F., Recognition and cooperation

between the ATP-dependent RNA helicase RhlB and ribonuclease RNase E. *Journal of molecular biology* **2007,** *367* (1), 113–132.

128. Liou, G.-G.; Chang, H.-Y.; Lin, C.-S.; Lin-Chao, S., DEAD box RhlB RNA helicase physically associates with exoribonuclease PNPase to degrade double-stranded RNA independent of the degradosome-assembling region of RNase E. *Journal of Biological Chemistry* **2002,** *277* (43), 41157–41162.

129. Tseng, Y.-T.; Chiou, N.-T.; Gogiraju, R.; Lin-Chao, S., The protein interaction of RNA helicase B (RhlB) and polynucleotide phosphorylase (PNPase) contributes to the homeostatic control of cysteine in Escherichia coli. *Journal of Biological Chemistry* **2015,** *290* (50), 29953–29963.

130. Redder, P.; Hausmann, S.; Khemici, V.; Yasrebi, H.; Linder, P., Bacterial versatility requires DEAD-box RNA helicases. *FEMS microbiology reviews* **2015**, fuv011.

131. Bizebard, T.; Ferlenghi, I.; Iost, I.; Dreyfus, M., Studies on three E. coli DEAD-box helicases point to an unwinding mechanism different from that of model DNA helicases. *Biochemistry* **2004,** *43* (24), 7857–7866.

132. Khemici, V.; Toesca, I.; Poljak, L.; Vanzo, N. F.; Carpousis, A. J., The RNase E of Escherichia coli has at least two binding sites for DEAD-box RNA helicases: Functional replacement of RhlB by RhlE. *Molecular microbiology* **2004,** *54* (5), 1422–1430.

133. Purusharth, R. I.; Klein, F.; Sulthana, S.; Jäger, S.; Jagannadham, M. V.; Evguenieva-Hackenberg, E.; Ray, M. K.; Klug, G., Exoribonuclease R interacts with endoribonuclease E and an RNA helicase in the psychrotrophic bacterium Pseudomonas syringae Lz4W. *Journal of Biological Chemistry* **2005,** *280* (15), 14572–14578.

134. Prud'homme-Généreux, A.; Beran, R. K.; Iost, I.; Ramey, C. S.; Mackie, G. A.; Simons, R. W., Physical and functional interactions among RNase E, polynucleotide phosphorylase and the cold-shock protein, CsdA: evidence for a 'cold shock degradosome'. *Molecular Microbiology* **2004,** *54* (5), 1409–1421.

135. Fu, A.; Tang, R.; Hardie, J.; Farkas, M. E.; Rotello, V. M., Promises and pitfalls of intracellular delivery of proteins. *Bioconjugate Chemistry* **2014,** *25* (9), 1602–1608.

136. Brock, R., The uptake of arginine-rich cell-penetrating peptides: putting the puzzle together. *Bioconjugate Chemistry* **2014,** *25* (5), 863–868.

137. Madani, F.; Lindberg, S.; Langel, Ü.; Futaki, S.; Gräslund, A., Mechanisms of cellular uptake of cell-penetrating peptides. *Journal of Biophysics* **2011,** *2011*.

138. Dubendorf, J. W.; Studier, F. W., Controlling basal expression in an inducible T7 expression system by blocking the target T7 promoter with lac repressor. *Journal of Molecular Biology* **1991,** *219* (1), 45–59.

139. Gossen, M.; Bujard, H., Tight control of gene expression in mammalian cells by tetracycline-responsive promoters. *Proceedings of the National Academy of Sciences* **1992,** *89* (12), 5547–5551.

140. Morales, D. P.; Braun, G. B.; Pallaoro, A.; Chen, R.; Huang, X.; Zasadzinski, J. A.; Reich, N. O., Targeted intracellular delivery of proteins with spatial and temporal control. *Molecular Pharmaceutics* **2014,** *12* (2), 600–609.

141. Guillard, S.; Minter, R. R.; Jackson, R. H., Engineering therapeutic proteins for cell entry: the natural approach. *Trends in Biotechnology* **2015,** *33* (3), 163–171.

142. Ryou, J.-H.; Sohn, Y.-K.; Hwang, D.-E.; Park, W.-Y.; Kim, N.; Heo, W.-D.; Kim, M.-Y.; Kim, H.-S., Engineering of bacterial exotoxins for highly efficient and receptor-specific intracellular delivery of diverse cargos. *Biotechnology and Bioengineering* **2016,** *113* (8), 1639–1646.

143. Krautz-Peterson, G.; Zhang, Y.; Chen, K.; Oyler, G. A.; Feng, H.; Shoemaker, C. B., Retargeting Clostridium difficile Toxin B to Neuronal Cells as a Potential Vehicle for Cytosolic Delivery of Therapeutic Biomolecules to Treat Botulism. *Journal of Toxicology* **2012,** *2012*, 9.

144. Verdurmen, W. P. R.; Luginbühl, M.; Honegger, A.; Plückthun, A., Efficient cell-specific uptake of binding proteins into the cytoplasm through engineered modular transport systems. *Journal of Controlled Release* **2015,** *200*, 13–22.

145. Kreitman, R. J.; Tallman, M. S.; Robak, T.; Coutre, S.; Wilson, W. H.; Stetler-Stevenson, M.; FitzGerald, D. J.; Lechleider, R.; Pastan, I., Phase I trial of anti-CD22 recombinant immunotoxin moxetumomab pasudotox (CAT-8015 or HA22) in patients with hairy cell leukemia. *Journal of Clinical Oncology* **2012,** *30* (15), 1822–1828.

146. Prince, H. M.; Duvic, M.; Martin, A.; Sterry, W.; Assaf, C.; Sun, Y.; Straus, D.; Acosta, M.; Negro-Vilar, A., Phase III placebo-controlled trial of denileukin diftitox for patients with cutaneous T-cell lymphoma. *Journal of Clinical Oncology* **2010,** *28* (11), 1870–1877.

147. Liou, J.-S.; Liu, B. R.; Martin, A. L.; Huang, Y.-W.; Chiang, H.-J.; Lee, H.-J., Protein transduction in human cells is enhanced by cell-penetrating peptides fused with an endosomolytic HA2 sequence. *Peptides* **2012,** *37* (2), 273–284.

148. Mechaly, A.; McCluskey, A. J.; Collier, R. J., Changing the receptor specificity of anthrax toxin. *MBio* **2012,** *3* (3), e00088–12.

149. Somm, E.; Bonnet, N.; Martinez, A.; Marks, P. M.; Cadd, V. A.; Elliott, M.; Toulotte, A.; Ferrari, S. L.; Rizzoli, R.; Hüppi, P. S., A botulinum toxin–derived targeted secretion inhibitor downregulates the GH/IGF1 axis. *The Journal of Clinical Investigation* **2012,** *122* (9), 3295–3306.

150. Kern, S. M.; Feig, A. L., Adaptation of Clostridium difficile toxin A for use as a protein translocation system. *Biochemical and Biophysical Research Communications* **2011,** *405* (4), 570–574.

151. Aktories, K., Self-cutting to kill: new insights into the processing of *Clostridium difficile* toxins. ACS Publications: **2007**.

152. Jank, T.; Aktories, K., Structure and mode of action of clostridial glucosylating toxins: the ABCD model. *Trends in Microbiology* **2008,** *16* (5), 222–229.

153. Chumbler, N. M.; Rutherford, S. A.; Zhang, Z.; Farrow, M. A.; Lisher, J. P.; Farquhar, E.; Giedroc, D. P.; Spiller, B. W.; Melnyk, R. A.; Lacy, D. B., Crystal structure of Clostridium difficile toxin A. *Nature Microbiology* **2016,** *1*.

154. Greco, A.; Ho, J. G.; Lin, S.-J.; Palcic, M. M.; Rupnik, M.; Ng, K. K., Carbohydrate recognition by Clostridium difficile toxin A. *Nature Structural & Molecular Biology* **2006,** *13* (5), 460–461.

155. Ho, J. G.; Greco, A.; Rupnik, M.; Ng, K. K.-S., Crystal structure of receptor-binding C-terminal repeats from *Clostridium difficile* toxin A. *Proceedings of the National Academy of Sciences of the United States of America* **2005,** *102* (51), 18373–18378.

156. Yin, J.; Straight, P. D.; McLoughlin, S. M.; Zhou, Z.; Lin, A. J.; Golan, D. E.; Kelleher, N. L.; Kolter, R.; Walsh, C. T., Genetically encoded short peptide tag for versatile protein labeling by Sfp phosphopantetheinyl transferase. *Proceedings of the National Academy of Sciences of the United States of America* **2005,** *102* (44), 15815–15820.

157. Tsukiji, S.; Nagamune, T., Sortase-Mediated Ligation: A Gift from Gram-Positive Bacteria to Protein Engineering. *ChemBioChem* **2009,** *10* (5), 787–798.

Abstract

Number of small RNA (sRNA) gene regulators have mounted in *E. coli* over the years whereas the number of validated protein partners has not changed considerably. Hfq has remained the only well studied global regulatory partner of sRNAs in *E. coli*. However, direct or indirect involvement of other protein partners has always been speculated. Study from Blasi lab has shown that CsdA, one of the five DEAD-box RNA helicases of *E. coli*, is required for the DsrA mediated upregulation of *rpoS* under cold stress condition. Previous study from our lab has identified two other DEAD-box RNA helicases, RhlB and RhlE, as potential protein partner of Hfq-sRNA mediated gene regulatory pathway. The work presented here was focused to investigate the plausible roles of RhlB and RhlE, DEAD-box helicases in Hfq-sRNA mediated regulatory pathways. In this study, using Hfq dependent sRNAs and their target mRNAs as substrates, we have shown that RhlB and RhlE both shows differential stimulation in substrate dependent manner; example: rA18 significantly simulates RhlE but fails to stimulate RhlB. Contrary to literature reports, significant ATPase activity has been observed for RhlB with several RNA substrates used in this study. However, consistent with literature reported observations, RhlE shows several folds higher stimulation of ATPase activity than the RhlB. Presence of Hfq has very little effects on the RhlE ATPase activity whereas the ATPase activity of RhlB was significantly modulated. While further investigation is needed, this study has shown that Hfq dependent sRNA and mRNA could significantly stimulate RhlB and RhlE, indicating towards the potential contribution of these helicases *in-vivo*.